Electronic Supplementary Material (ESI) for Dalton Transactions.
This journal is © The Royal Society of Chemistry 2019

Electronic Supplementary Information for

Bimetallic and trimetallic zinc amino-bis(phenolate) complexes for ring-opening polymerization of *rac*-lactide

Yi Liu[a], Louise N. Dawe[b] and Christopher M. Kozak*[,a]

[a] Department of Chemistry, Memorial University of Newfoundland, St. John's, Newfoundland, Canada A1B 3X7. E-mail: ckozak@mun.ca.

[b] Department of Chemistry and Biochemistry, Wilfrid Laurier University, 75 University Ave. W. Waterloo, Ontario, N2L 3C5, Canada

Crystallographic Experimental S4
Table S1. Crystal data and structure refinement for **1a·THF** and **3**. S4
Table S2. Melt phase ROP of *rac*-LA using complex **1a**, T=125 °C. S6
Figure S1. Plots of monomer conversion vs. time (top) and $\ln[LA]_0/[LA]_t$ vs. time excluding induction period (bottom) for ROP of *rac*-lactide catalyzed by complex **1a** ([LA]:[**1a**] = 100:1, [LA] = 0.11 M in toluene-d_8, 80 °C). The solid lines are the best linear fits. 5
Figure S2. Monomer conversion vs. time for melt phase ROP of *rac*-LA catalyzed by complex **1a** ([LA]:[**1a**] = 200:1, 130 °C). 6
Figure S3. First order plot of $\ln[LA]_0/[LA]_t$ vs. time for melt phase ROP of *rac*-LA catalyzed by complex **1a** ([LA]:[**1a**] = 200:1, 130 °C). 6
Figure S4. Plots of $\ln[LA]_0/[LA]_t$ vs. time for ROP of *rac*-LA catalyzed by complex **1a·THF**/BnOH and **1a** /BnOH ([LA]:[complex]:[BnOH] = 200:1:1, [LA] = 0.66 M in toluene-d_8, 80 °C) 7
Figure S5. MALDI mass spectra of PLA (A: linear mode; B: reflectron mode; C: experimental vs. calculated isotopic distributions) obtained using complex **1a** ([LA]:[**1a**] = 100:1, 130 °C) 8
Figure S6. Observed rate constant k_{obs} vs. [Polymer chains]:[Complex] plot (bottom) for the ROP of *rac*-LA catalyzed by **1a·THF**/BnOH (where [LA]:[**1a·THF**]: [BnOH] = 200:1:1, 200:1:2 and 200:1:5; [LA] = 0.66 M in toluene-d_8 at 80 °C). The solid line is the best linear fit to the equation shown. 9
Figure S7. Plot of M_n (GPC) vs. [LA]:[**1a·THF**] for ROP of *rac*-LA catalyzed by **1a·THF**/BnOH (where [LA]:[**1a·THF**]:[BnOH] = 100:1:1, 200:1:1 and 500:1:1; [LA] = 0.66 M in toluene-d_8 at 80 °C) 9
Figure S8. Plot of M_n (GPC) vs. [LA]:[BnOH] for ROP of *rac*-LA catalyzed by **1a·THF**/BnOH (where [LA]:[**1a·THF**]:[BnOH] = 200:1:1, 200:1:2 and 200:1:5; [LA] = 0.66 M in toluene-d_8 at 80 °C) 10
Figure S9. MALDI mass spectrum (linear mode) of PLA obtained using complex **1a·THF** ([LA]:[**1a·THF**]:[BnOH] = 100:1:1, 80 °C in toluene), (**I**: full spectrum; **II**: expanded spectrum with experimental calculated peaks) 11

Figure S10. MALDI-TOF mass spectrum (reflectron mode) of PLA obtained using complex **1a·THF** ([LA]:[**1a·THF**] :[BnOH] = 100:1:1, 80 °C in toluene), (**I**: full spectrum; **II**: expanded spectrum with experimental and calculated peaks). 12
Figure S11. MALDI-TOF mass spectrum (linear mode) of PLA obtained using complex **1a·THF** ([LA]:[**1a·THF**] :[BnOH] = 500:1:1, 80 °C in toluene), (**I**: full spectrum; **II**: expanded spectrum with experimental and calculated peaks). 13
Figure S12. MALDI-TOF mass spectrum (reflectron mode) of PLA obtained using complex **1a·THF** ([LA]:[**1a·THF**] :[BnOH] = 500:1:1, 80 °C in toluene), (**I**: full spectrum; **II**: expanded spectrum with experimental and calculated peaks). 14
Figure S13. First order plots of $\ln[LA]_0/[LA]_t$ vs. time for ROP of *rac*-LA catalyzed by complex **3**/*i*-PrOH or /BnOH ([LA]:[**3**]:[*i*-PrOH] = 100:1:1 and 100:1:5; [LA]:[**3**]:[BnOH] = 100:1:1 and 100:1:5; [LA] = 0.66 M in toluene-d_8, 80 °C). 15
Figure S14. First order plots of $\ln[LA]_0/[LA]_t$ vs. time and corresponding Arrhenius plot of $\ln k_{obs}$ vs. 1/T for ROP of *rac*-LA catalyzed by **3**/BnOH ([LA]:[**3**]:[BnOH] = 100:1:1, [LA] = 0.66 M in toluene-d_8) in the temperature range of 70 to 90 °C. The solid line is the best linear fit. 16
Figure S15. Eyring plot for ROP of *rac*-LA catalyzed by complex **3**/BnOH ([LA]:[**3**]:[BnOH] = 100:1:1, [LA] = 0.66 M in toluene-d_8) in the temperature range of 70 to 90 °C. The solid line is the best linear fit. 17
Figure S16. First order plots of $\ln[LA]_0/[LA]_t$ vs. time (left) and corresponding observed rate constant k_{app} vs. [Polymer chains]:[Complex] plots (right) for the immortal ROP of *rac*-LA catalyzed by complex **3**/*i*-PrOH to determine the dependence on [*i*-PrOH]([LA]:[**3**]:[*i*-PrOH] = 100:1:1, 5, 10; [LA] = 0.66 M in toluene-d_8, 80 °C). The solid lines are the best linear fits. 17
Figure S17. MALDI mass spectra of PLA (top: linear mode expanded spectrum with theoretically modelled peaks; bottom: reflectron mode) obtained using complex **3**/*i*-PrOH ([LA]:[**3**]:[*i*-PrOH] = 100:1:1, [LA] = 0.66 M in toluene-d_8, 90 °C) 18
Figure S18. MALDI mass spectra and expanded spectrum with theoretically modelled peaks of PLA (linear mode) obtained using complex **3**/BnOH ([LA]:[**3**]:[BnOH] = 100:1:1, [LA] = 0.66 M in toluene-d_8, 80 °C) 19
Figure S19. ^{1}H NMR spectra in toluene-d_8 of A: BnOH; B: *ra*c-LA and BnOH (1:1 ratio) following heating to 353 K then cooling to 298 K; and C: *ra*c-LA 20
Figure S20. ^{1}H NMR spectra in toluene-d_8 of A: **1a·THF**; B: **1a·THF** with one equivalent BnOH; C: **1a·THF** with two equivalents BnOH. 21
Figure S21. Complete ^{1}H NMR spectra (top), expansion of the THF peak region (bottom-left), and expansion of the ethyl group region (bottom-right) in toluene-d_8. A: [LA]:[**1a·THF**]:[BnOH] = 1:1:1 after heating to 353 K for 60 min; B: mixture of [LA]:[**1a·THF**]:[BnOH] = 1:1:1 before heating; C: **1a·THF** alone. 22
Figure S22. ^{1}H NMR spectra (top) and expanded spectra of ethyl group region (bottom), in toluene-d_8. A: [LA]:[**1a·THF**]:[BnOH] = 1:1:2 after heating for 72 min; B: mixture of [LA]:[**1a·THF**]:[BnOH] = 1:1:2 before heating; C: **1a·THF**. 23

Figure S23. Expanded ^{1}H NMR spectra in toluene-d_8 of A: [LA]:[**1a·THF**]:[BnOH] = 1:1:1 after heating for 72 min; B: mixture of [LA]:[**1a·THF**]:[BnOH] = 1:1:2 after heating for 60 min; C: mixture of [LA]:[**1a·THF**]:[BnOH] = 2:1:1 after heating for 60 min. 24
Figure S24. ^{1}H NMR spectra in toluene-d_8, of A: **1a·THF** with one equivalent of BnOH; B: **1a·THF** with one equivalent BnOH then addition of one equivalent of LA; C: the mixture of B after heating for 1h. 25
Figure S25. ^{1}H NMR spectrum of **1a** (300 MHz, $CDCl_3$, 298 K). 26
Figure S26. ^{13}C NMR spectum of **1a**, (75.5 MHz, $CDCl_3$, 298 K). 26
Figure S27. APT (attached proton test) spectrum of **1a** (75.5 MHz, $CDCl_3$, 298 K).....27
Figure S28. ^{1}H NMR spectrum of **1b** (300 MHz, $CDCl_3$, 298 K).....27
Figure S29. ^{13}C NMR spectrum of **1b** (75.5 MHz, $CDCl_3$, 298 K)……...28
Figure S30. ^{1}H NMR spectrum of **1a·THF** (300 MHz, $CDCl_3$, 298 K). 28
Figure S31. COSY (correlation spectroscopy) spectrum of **1a·THF**, (300 MHz, $CDCl_3$, 298 K). 29
Figure S32. ^{1}H NMR spectrum of **1a·THF** (300 MHz, toluene-d_8, 298 K).....29
Figure S33. ^{13}C NMR spectrum of **1a·THF** (75.5 MHz, $CDCl_3$, 298 K). 30
Figure S34. ^{1}H NMR spectrum of **3** (300 MHz, $CDCl_3$, 298 K). 30
Figure S35. ^{1}H NMR spectrum of **4** (300 MHz, pyridine-d_5, 298 K).....31
Figure S36. COSY (correlation spectroscopy) spectrum of **3** (300 MHz, $CDCl_3$, 298 K).....31
Figure S37. ^{13}C NMR spectrum of **3** (75.5 MHz, $CDCl_3$, 298 K). 32
Figure S38. HSQC (heteronuclear single quantum coherence spectroscopy) spectrum of **3** (300 MHz, $CDCl_3$, 298 K). 32
Figure S39. Homonuclear decoupled ^{1}H NMR spectrum of the methine region of PLA prepared from *rac*-LA with **1a·THF**/BnOH ([LA]:[**1a·THF**]:[BnOH]=100:1:1), at 80 °C for 40 min. (500 MHz, $CDCl_3$). 33

Crystallographic Experimental

Measurements were made on a Bruker APEXII CCD equipped diffractometer (30 mA, 50 kV) using monochromated Mo Kα radiation (λ = 0.71073 Å) at 125 K by Prof. Jason Masuda (Chemistry Department, St. Mary's University, Halifax, Nova Scotia, Canada). Refinement of the data was performed by Prof. Louise N. Dawe (Department of Chemistry and Biochemistry, Wilfrid Laurier University, Waterloo, Ontario, Canada). Structures were solved using Olex2[1], the structure was solved with the ShelXT[2] structure solution program using Direct Methods and refined with the ShelXL[3] refinement package using Least Squares minimisation. H-atoms were introduced in calculated positions and refined on a riding model, while all other atoms were introduced in difference map positions and refined anisotropically. For **3**, two disordered t-butyl groups are present. C56-C58:C56A-C58A at 0.581(8):0.419(8) occupancy and C60-C62:C60A-C62A at 0.731(8):0.269(8) occupancy. Both groups were refined anisotropically with SADI and RIGU restraints. All other non-hydrogen atoms were refined anisotropically, without restraints.

1. Dolomanov, O.V., Bourhis, L.J., Gildea, R.J, Howard, J.A.K. & Puschmann, H. (2009), J. Appl. Cryst. 42, 339-341.
2. Sheldrick, G.M. (2008). Acta Cryst. A64, 112-122.
3. Sheldrick, G.M. (2008). Acta Cryst. A64, 112-122.

Table S1. Crystal data and structure refinement for **1a·THF** and **3**.

Complex	**1a·THF**	**3**
Empirical formula	$C_{41}H_{69}NO_3Zn_2$	$C_{72}H_{116}N_2O_6Zn_3$
Formula weight	754.71	1301.77
Temperature/K	125.03	125.02
Crystal system	monoclinic	Monoclinic
Space group	$P2_1/c$	$P2_1/c$
a/Å	12.9102(11)	13.4644(9)
b/Å	10.9571(10)	28.1652(19)
c/Å	28.288(3)	20.0841(14)
α/°	90	90
β/°	93.6070(10)	104.2080(10)
γ/°	90	90
Volume/Å^3	3993.6(6)	7383.5(9)
Z	4	4
ρ_{calc}g/cm^3	1.255	1.171
μ/mm^{-1}	1.237	1.014
F(000)	1624.0	2800.0
Crystal size/mm^3	0.401 × 0.335 × 0.231	0.354 × 0.251 × 0.226
Radiation	MoKα (λ = 0.71073)	MoKα (λ = 0.71073)
2Θ range for data collection/°	3.988 to 57.406	4.184 to 56.584
Index ranges	$-16 \le h \le 16$, $-14 \le k \le 12$, $-37 \le l \le 38$	$-17 \le h \le 17$, $-36 \le k \le 37$, $-26 \le l \le 24$
Reflections collected	31734	60031

Independent reflections	9708 [R_{int} = 0.0263, R_{sigma} = 0.0292]	17705 [R_{int} = 0.0533, R_{sigma} = 0.0621]
Data/restraints/parameters	9708/0/439	17705/102/840
Goodness-of-fit on F^2	1.027	1.013
R_1, wR_2 [I>=2σ (I)]	0.0289, 0.0683	0.0426, 0.0871
R_1, wR_2 [all data]	0.0382, 0.0721	0.0805, 0.0995
Largest diff. peak/hole / e $Å^{-3}$	0.37/-0.22	0.41/-0.40
CCDC Reference	1412177	1412178

[a] $R_1 = \Sigma(|F_o| - |F_c|)/\Sigma|F_o|$; $wR_2 = [\Sigma/(w(F_o^2 - F_c^2)^2)/\Sigma w(F_o^2)^2]^{1/2}$, where $w = 1/\sigma^2(F_o^2) + (aP)^2 + bP$.

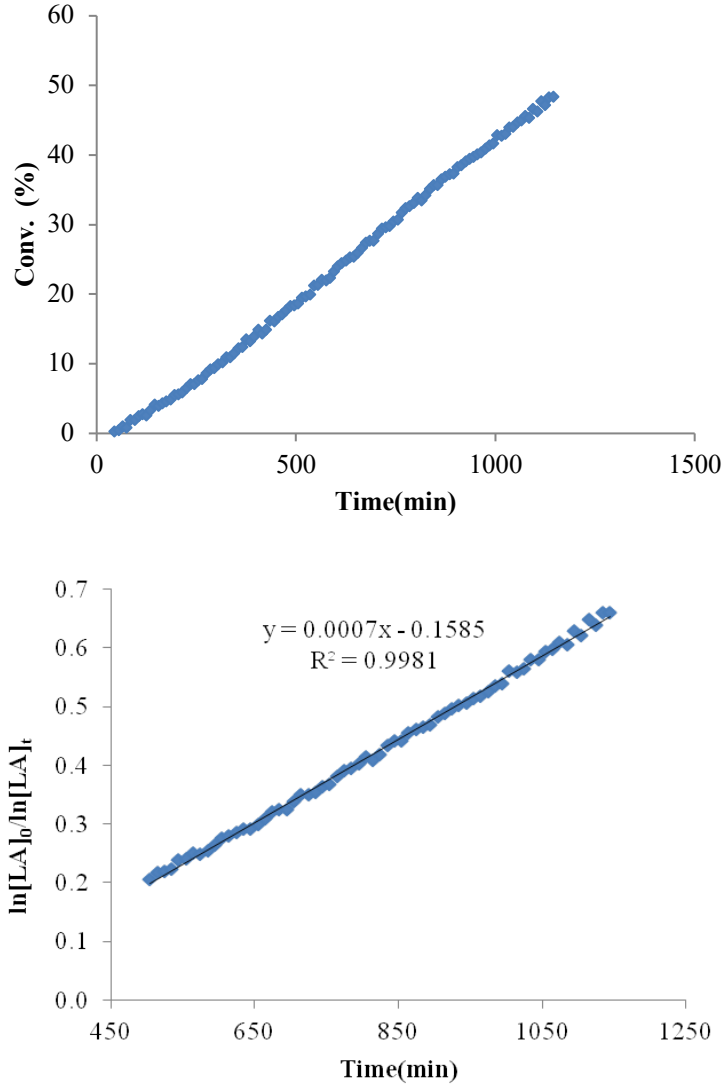

Figure S1. Plots of monomer conversion vs. time (top) and $\ln[LA]_0/[LA]_t$ vs. time excluding induction period (bottom) for ROP of *rac*-lactide catalyzed by complex **1a** ([LA]:[**1a**] = 100:1, [LA] = 0.11 M in toluene-d_8, 80 °C). The solid lines are the best linear fits.

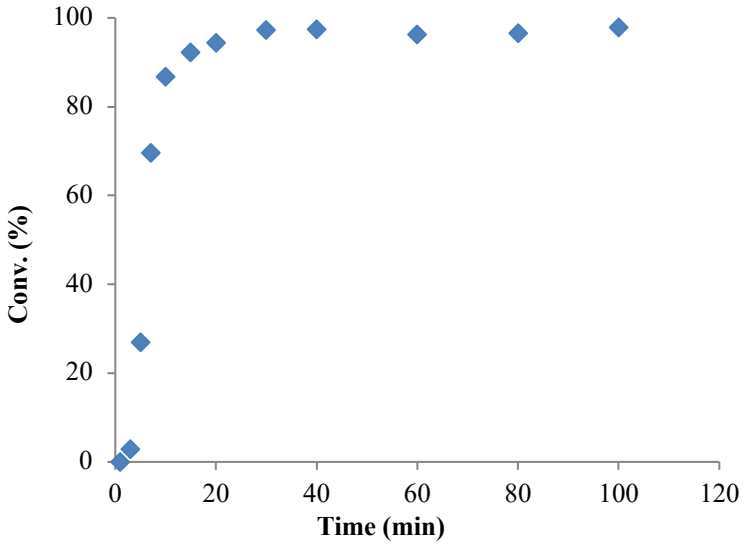

Figure S2. Monomer conversion vs. time for melt phase ROP of *rac*-LA catalyzed by complex **1a** ([LA]:[**1a**] = 200:1, 130 °C).

Table S2. Melt phase ROP of *rac*-LA using complex **1a**, T = 125 °C.

Entry	[LA]:[1a]	Time (min)	Conv. (%)*
1	100:1	100	98.4
2	200:1	100	97.6
3	500:1	100	64.7
4	1000:1	100	17.4

*Calculated via integration of the methine resonances of lactide and polylactide

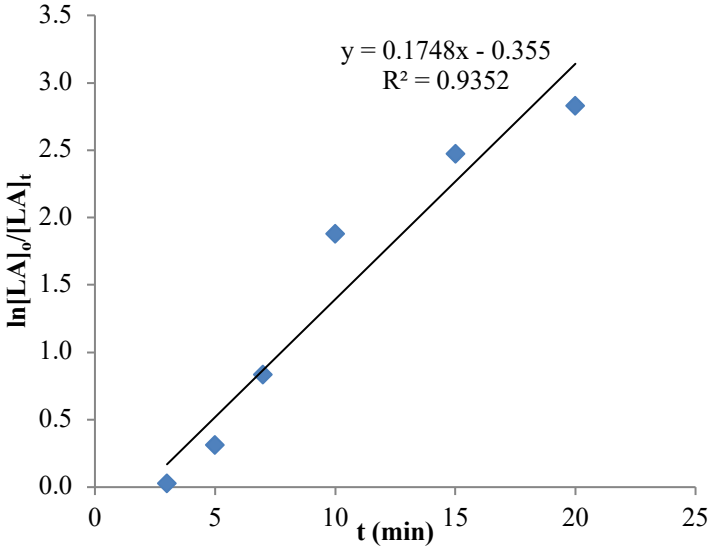

Figure S3. First order plot of $\ln[LA]_0/[LA]_t$ vs. time for melt phase ROP of *rac*-LA catalyzed by complex **1a** ([LA]:[**1a**] = 200:1, 130 °C).

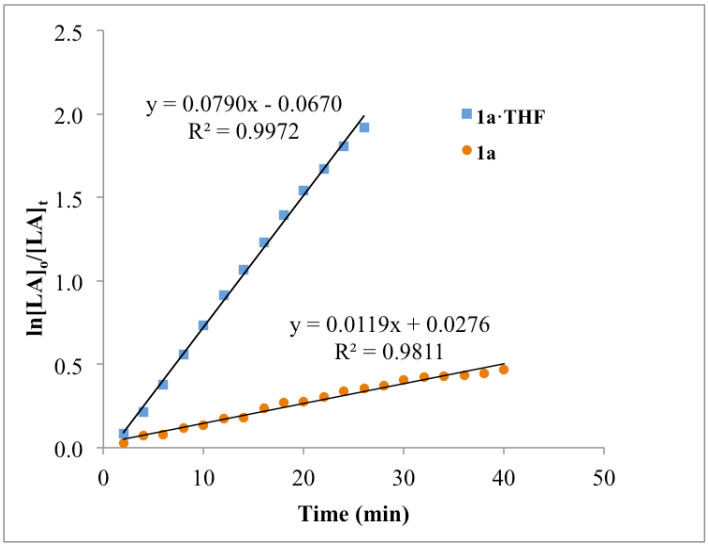

Figure S4. Plots of $\ln[LA]_0/[LA]_t$ vs. time for ROP of *rac*-LA catalyzed by complex **1a·THF**/BnOH and **1a** /BnOH ([LA]:[complex]:[BnOH] = 200:1:1, [LA] = 0.66 M in toluene-d_8, 80 °C).

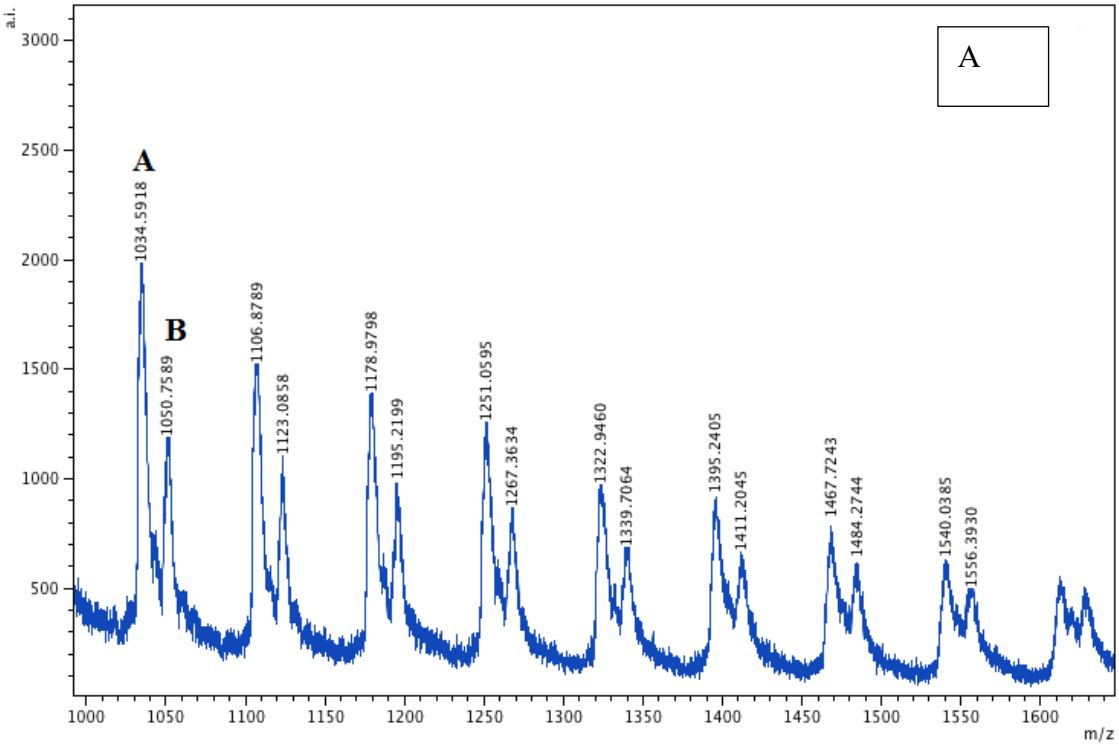

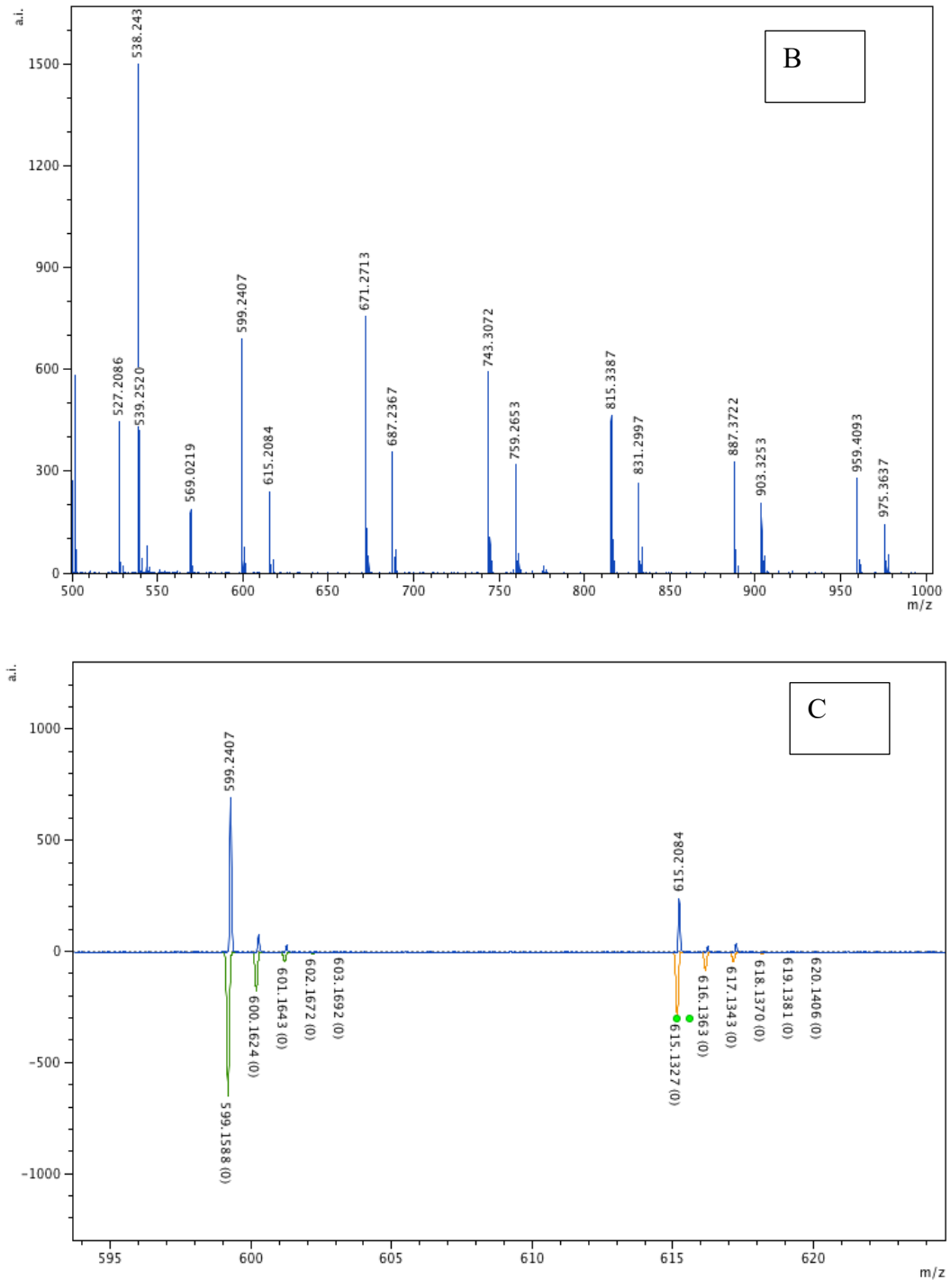

Figure S5. MALDI mass spectra of PLA (A: linear mode; B: reflectron mode; C: experimental vs. calculated isotopic distributions) obtained using complex **1a** ([LA]:[**1a**] = 100:1, 130 °C).

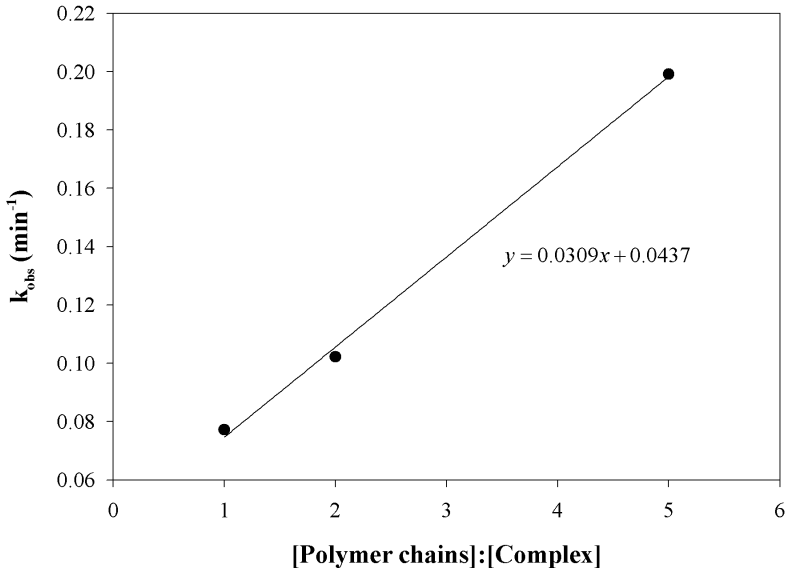

Figure S6. Observed rate constant k_{obs} vs. [Polymer chains]:[Complex] plot (bottom) for the ROP of *rac*-LA catalyzed by **1a·THF**/BnOH (where [LA]:[**1a·THF**]: [BnOH] = 200:1:1, 200:1:2 and 200:1:5; [LA] = 0.66 M in toluene-d_8 at 80 °C). The solid line is the best linear fit to the equation shown.

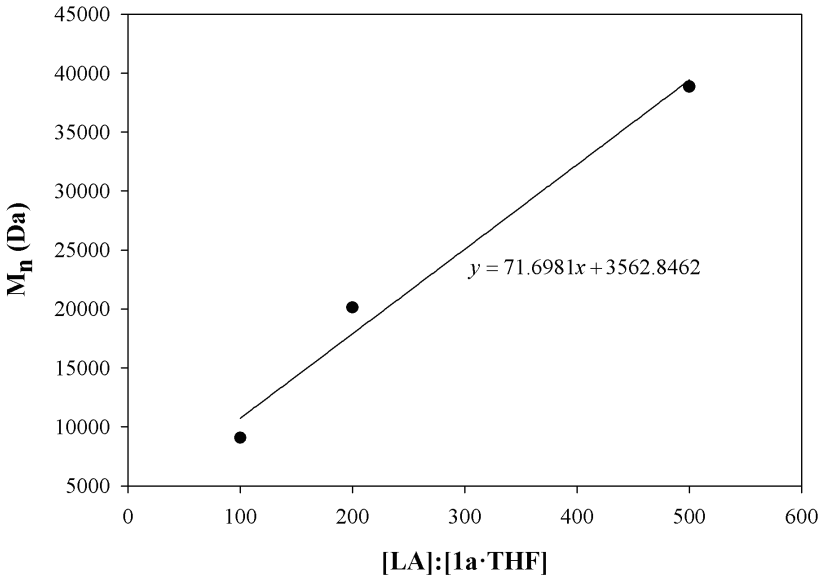

Figure S7. Plot of M_n (GPC) vs. [LA]:[**1a·THF**] for ROP of *rac*-LA catalyzed by **1a·THF**/BnOH (where [LA]:[**1a·THF**]:[BnOH] = 100:1:1, 200:1:1 and 500:1:1; [LA] = 0.66 M in toluene-d_8 at 80 °C).

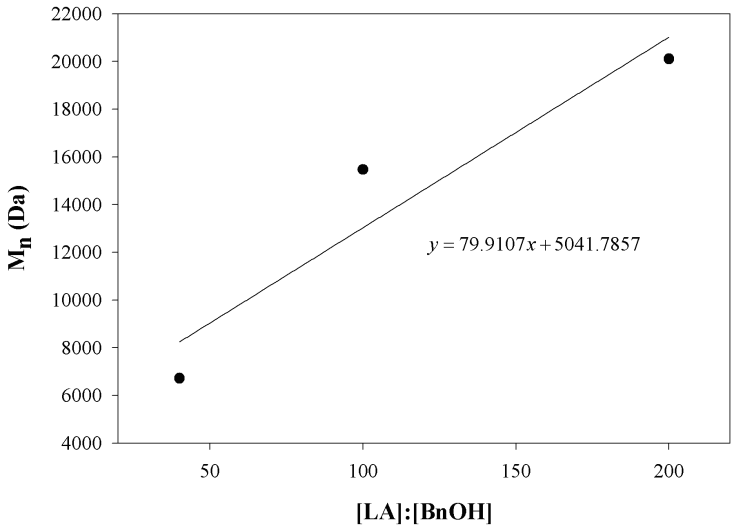

Figure S8. Plot of M_n (GPC) vs. [LA]:[BnOH] for ROP of *rac*-LA catalyzed by **1a·THF**/BnOH (where [LA]:[**1a·THF**]:[BnOH] = 200:1:1, 200:1:2 and 200:1:5; [LA] = 0.66 M in toluene-d_8 at 80 °C).

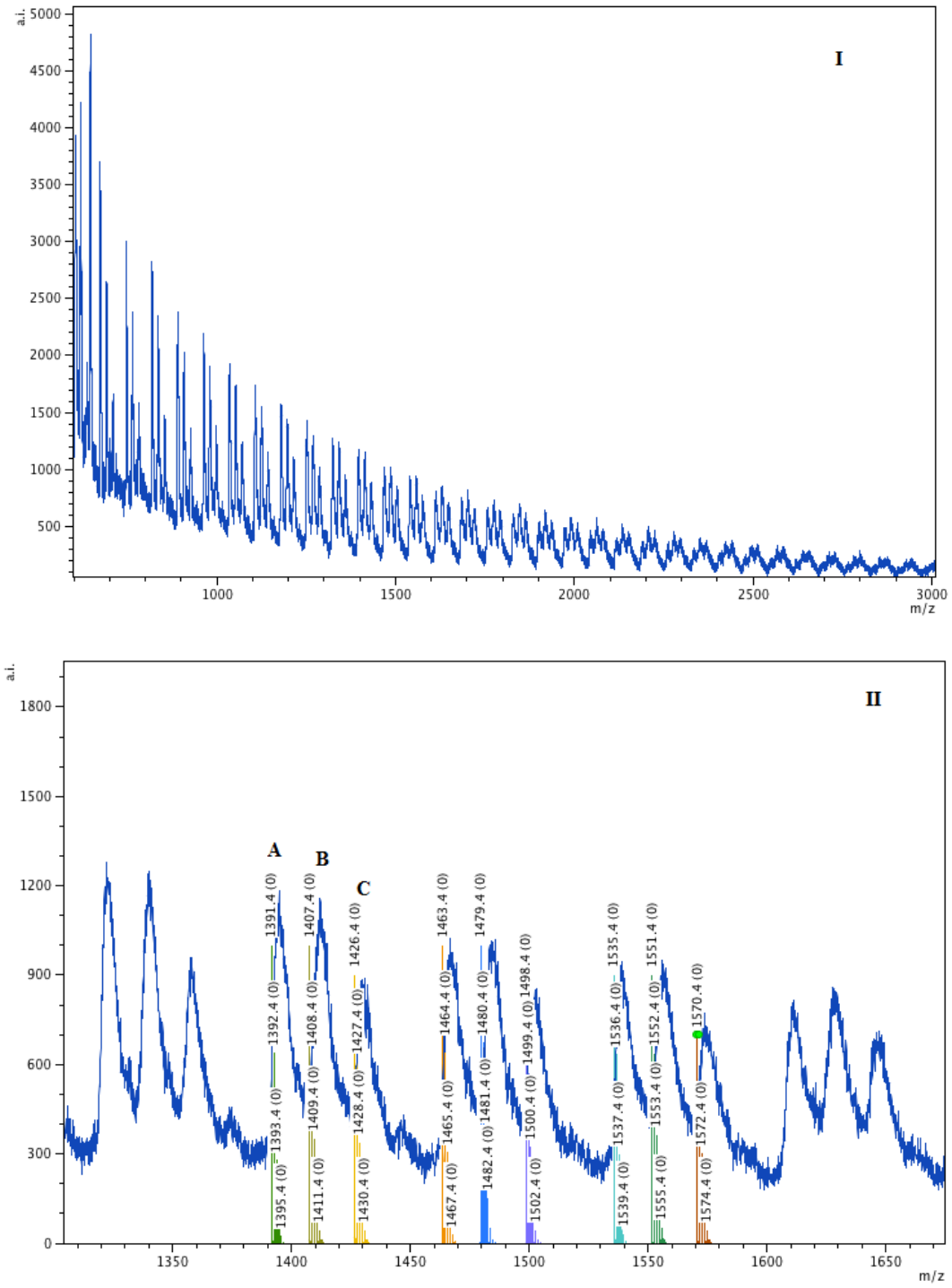

Figure S9. MALDI mass spectrum (linear mode) of PLA obtained using complex **1a·THF** ([LA]:[**1a·THF**]:[BnOH] = 100:1:1, 80 °C in toluene), (**I**: full spectrum; **II**: expanded spectrum with experimental calculated peaks).

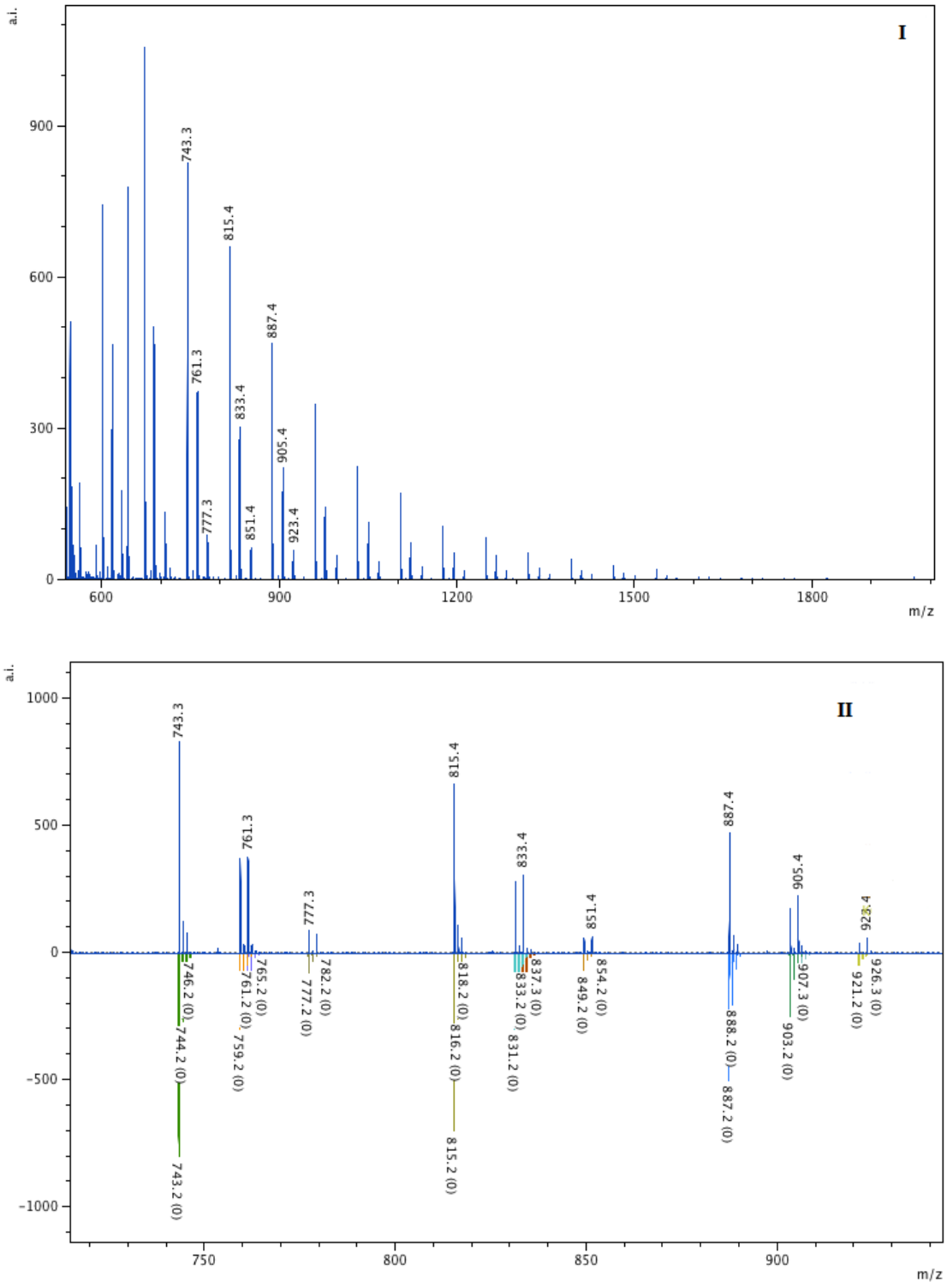

Figure S10. MALDI-TOF mass spectrum (reflectron mode) of PLA obtained using complex **1a·THF** ([LA]:[**1a·THF**] :[BnOH] = 100:1:1, 80 °C in toluene), (**I**: full spectrum; **II**: expanded spectrum with experimental and calculated peaks).

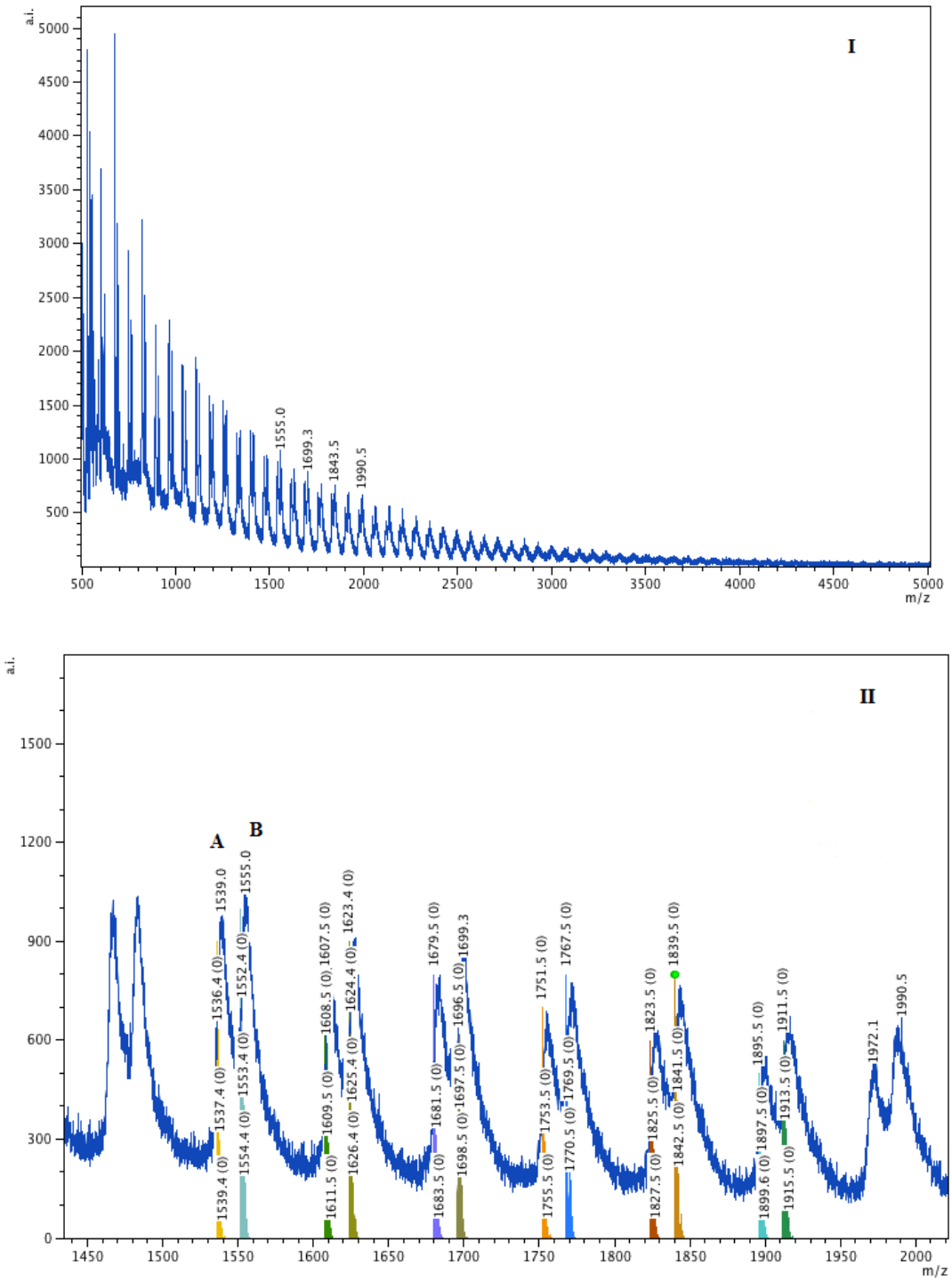

Figure S11. MALDI-TOF mass spectrum (linear mode) of PLA obtained using complex **1a·THF** ([LA]:[**1a·THF**] :[BnOH] = 500:1:1, 80 °C in toluene), (**I**: full spectrum; **II**: expanded spectrum with experimental and calculated peaks).

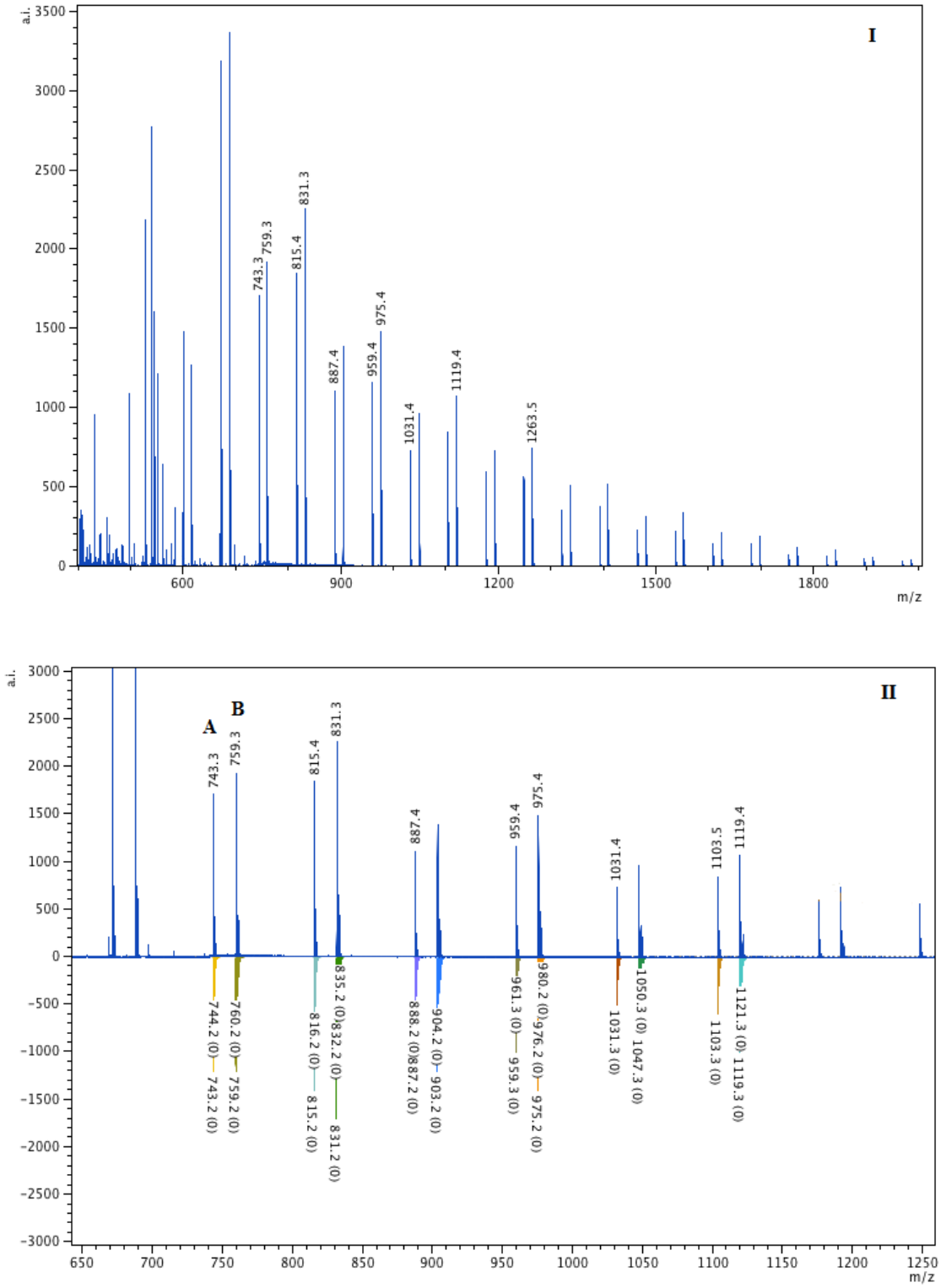

Figure S12. MALDI-TOF mass spectrum (reflectron mode) of PLA obtained using complex **1a·THF** ([LA]:[**1a·THF**] :[BnOH] = 500:1:1, 80 °C in toluene), (**I**: full spectrum; **II**: expanded spectrum with experimental and calculated peaks).

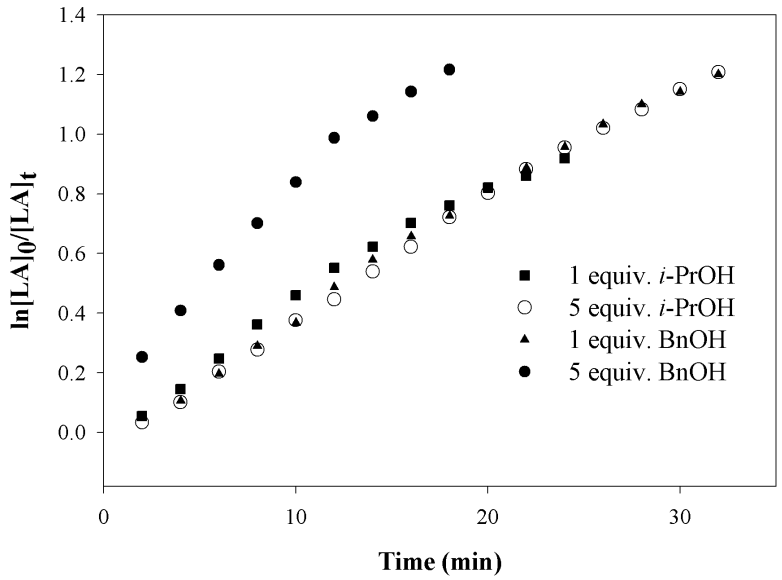

Figure S13. First order plots of $\ln[LA]_0/[LA]_t$ vs. time for ROP of *rac*-LA catalyzed by complex **3**/*i*-PrOH or /BnOH ([LA]:[**3**]:[*i*-PrOH] = 100:1:1 and 100:1:5; [LA]:[**3**]:[BnOH] = 100:1:1 and 100:1:5; [LA] = 0.66 M in toluene-d_8, 80 °C).

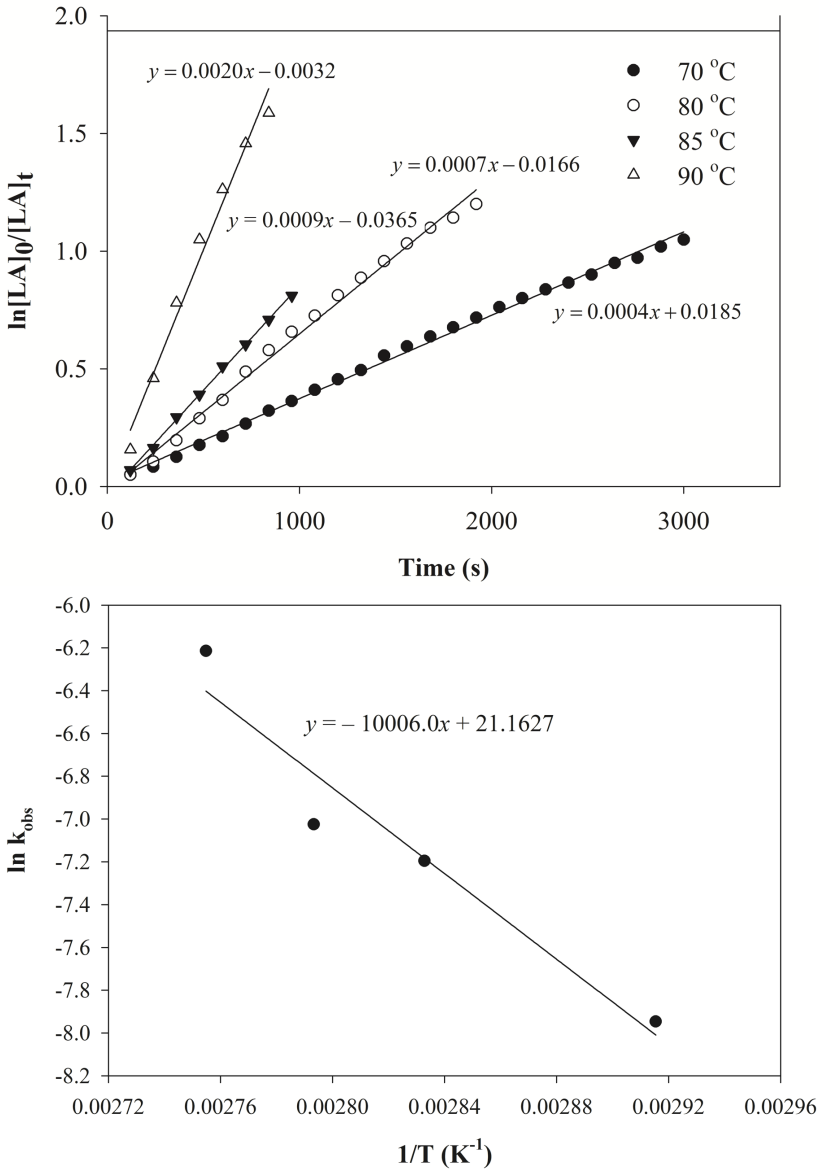

Figure S14. First order plots of $\ln[LA]_0/[LA]_t$ vs. time and corresponding Arrhenius plot of $\ln k_{obs}$ vs. 1/T for ROP of *rac*-LA catalyzed by **3**/BnOH ([LA]:[**3**]:[BnOH] = 100:1:1, [LA] = 0.66 M in toluene-d_8) in the temperature range of 70 to 90 °C. The solid line is the best linear fit.

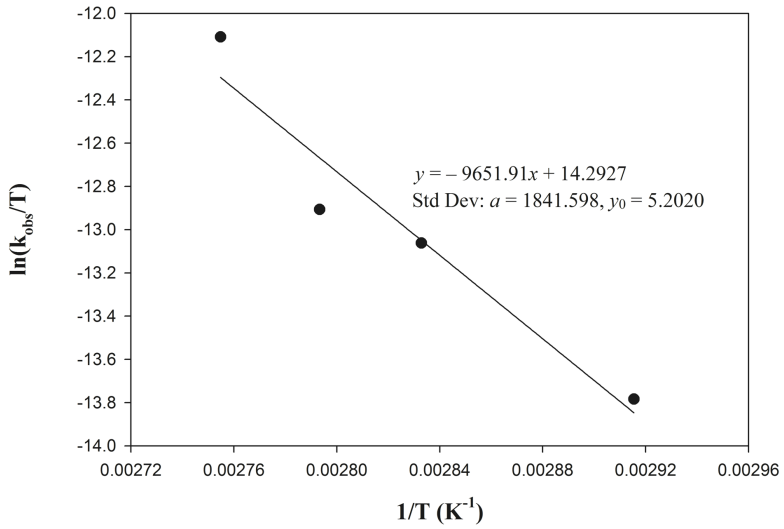

Figure S15. Eyring plot for ROP of *rac*-LA catalyzed by complex **3**/BnOH ([LA]:[**3**]:[BnOH] = 100:1:1, [LA] = 0.66 M in toluene-d_8) in the temperature range of 70 to 90 °C. The solid line is the best linear fit.

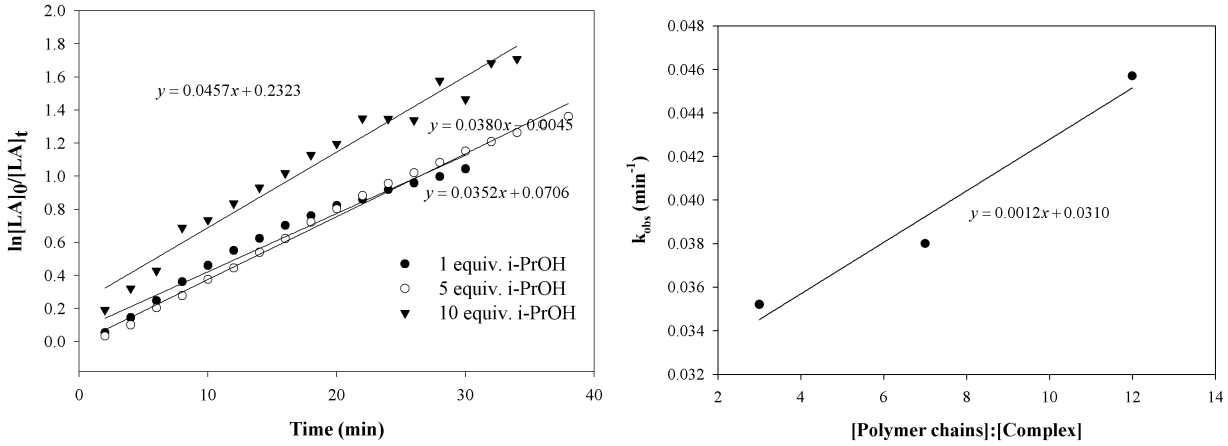

Figure S16. First order plots of $\ln[LA]_0/[LA]_t$ vs. time (left) and corresponding observed rate constant k_{app} vs. [Polymer chains]:[Complex] plots (right) for the immortal ROP of *rac*-LA catalyzed by complex **3**/*i*-PrOH to determine the dependence on [*i*-PrOH]([LA]:[**3**]:[*i*-PrOH] = 100:1:1, 5, 10; [LA] = 0.66 M in toluene-d_8, 80 °C). The solid lines are the best linear fits.

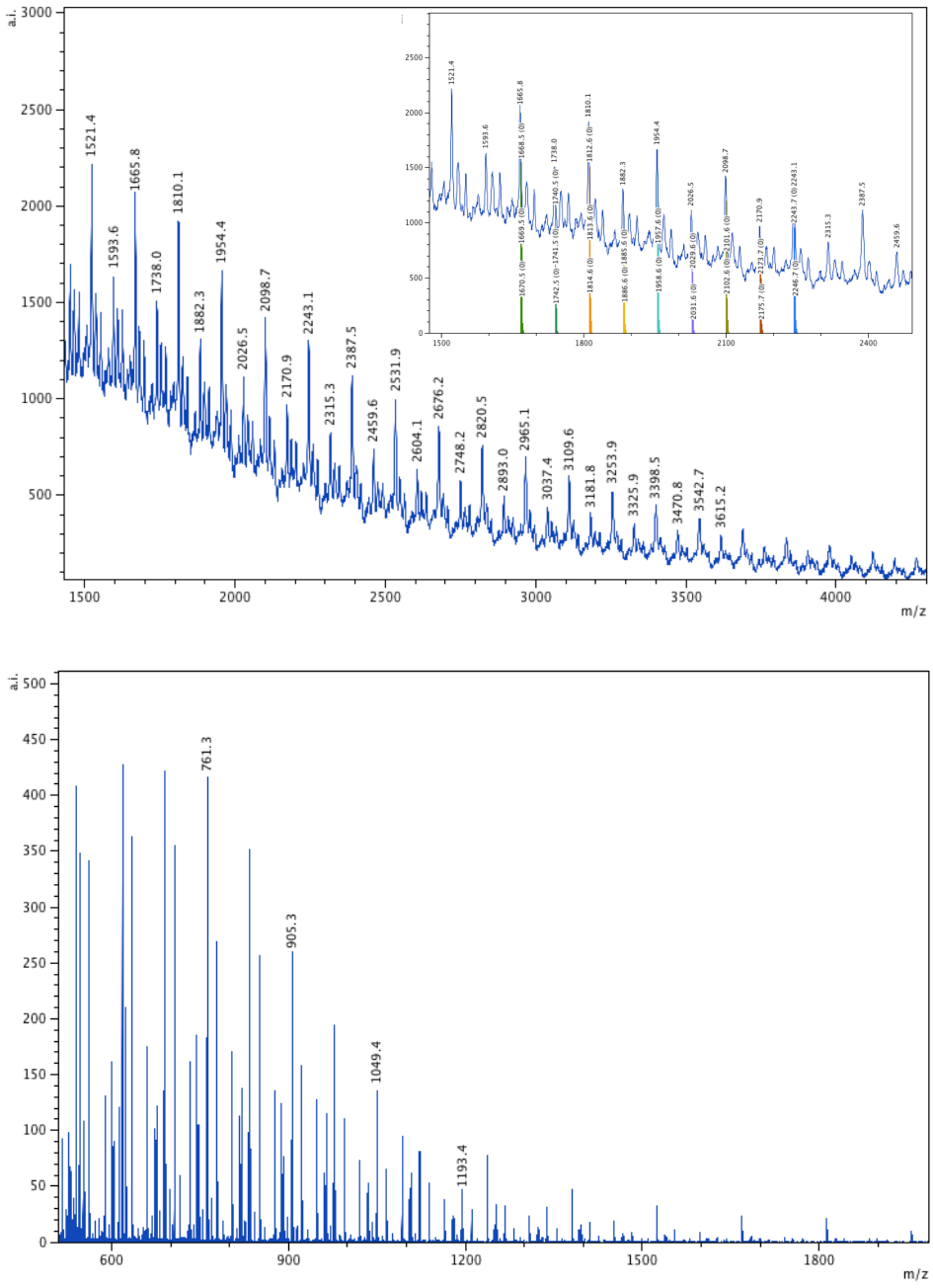

Figure S17. MALDI mass spectra of PLA (top: linear mode expanded spectrum with theoretically modelled peaks; bottom: reflectron mode) obtained using complex **3**/*i*-PrOH ([LA]:[**3**]:[*i*-PrOH] = 100:1:1, [LA] = 0.66 M in toluene-d_8, 90 °C)

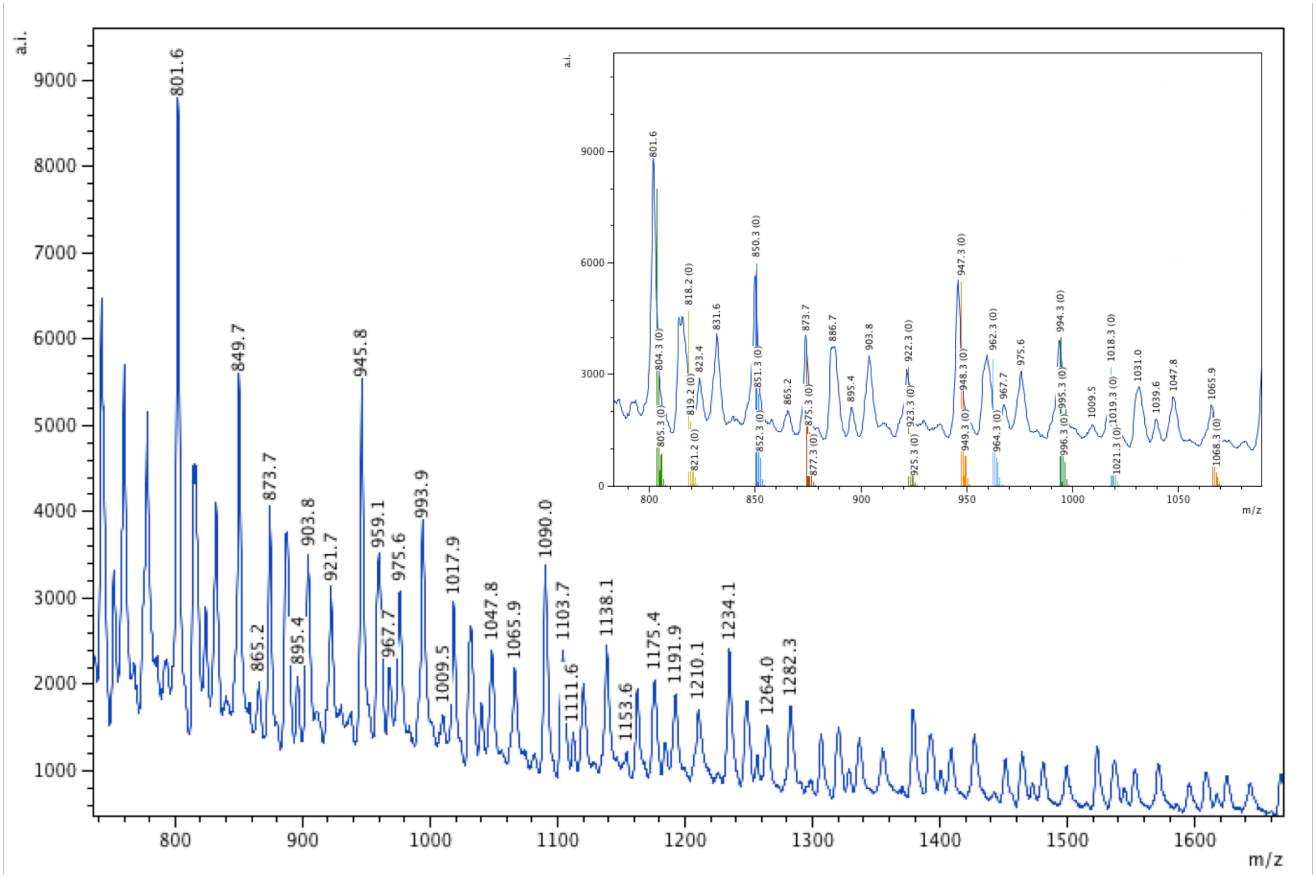

Figure S18. MALDI mass spectra and expanded spectrum with theoretically modelled peaks of PLA (linear mode) obtained using complex **3**/BnOH ([LA]:[**3**]:[BnOH] = 100:1:1, [LA] = 0.66 M in toluene-d_8, 80 °C)

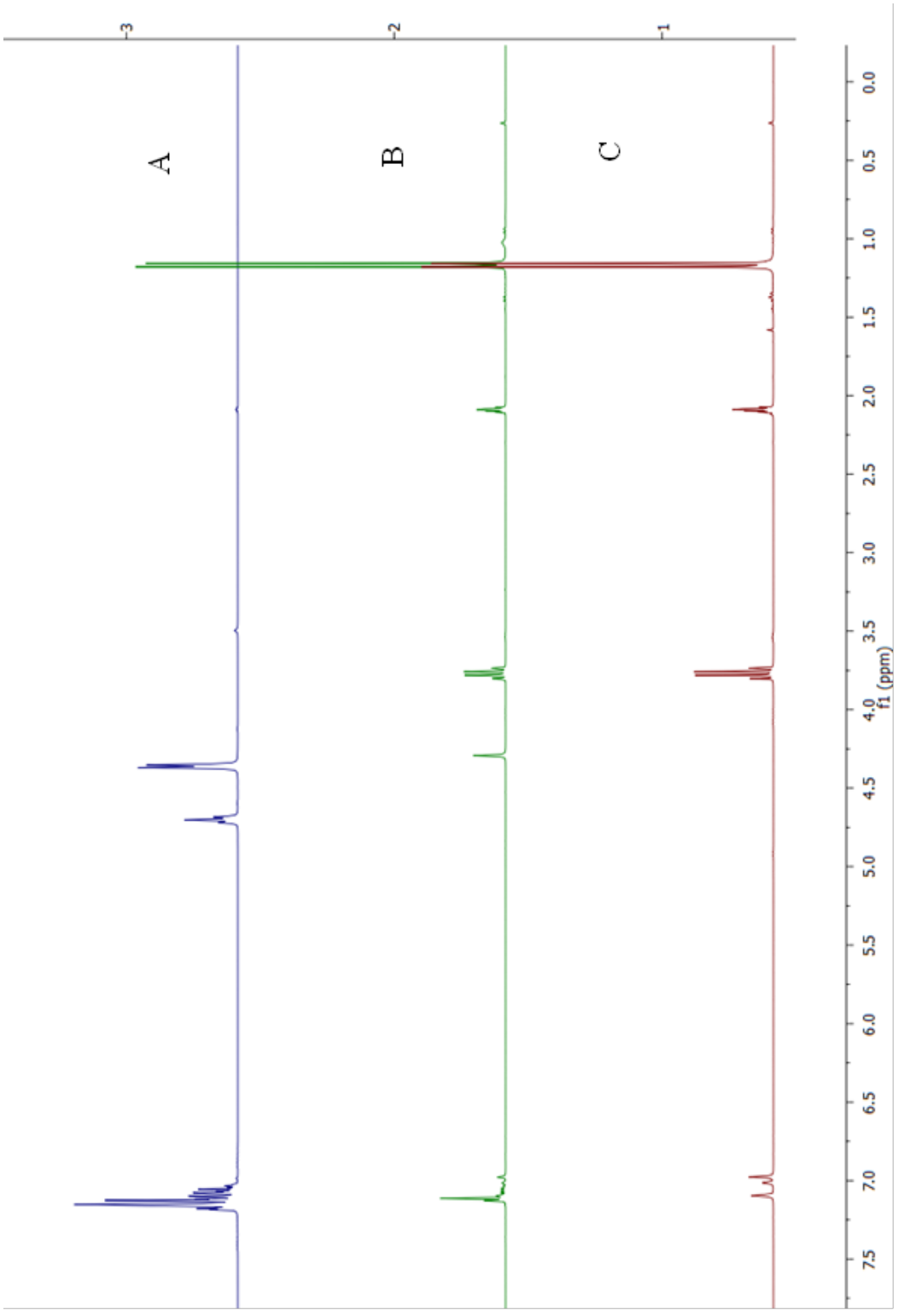

Figure S19. ^{1}H NMR spectra in toluene-d_8 of A: BnOH; B: *rac*-LA and BnOH (1:1 ratio) following heating to 353 K then cooling to 298 K; and C: *rac*-LA

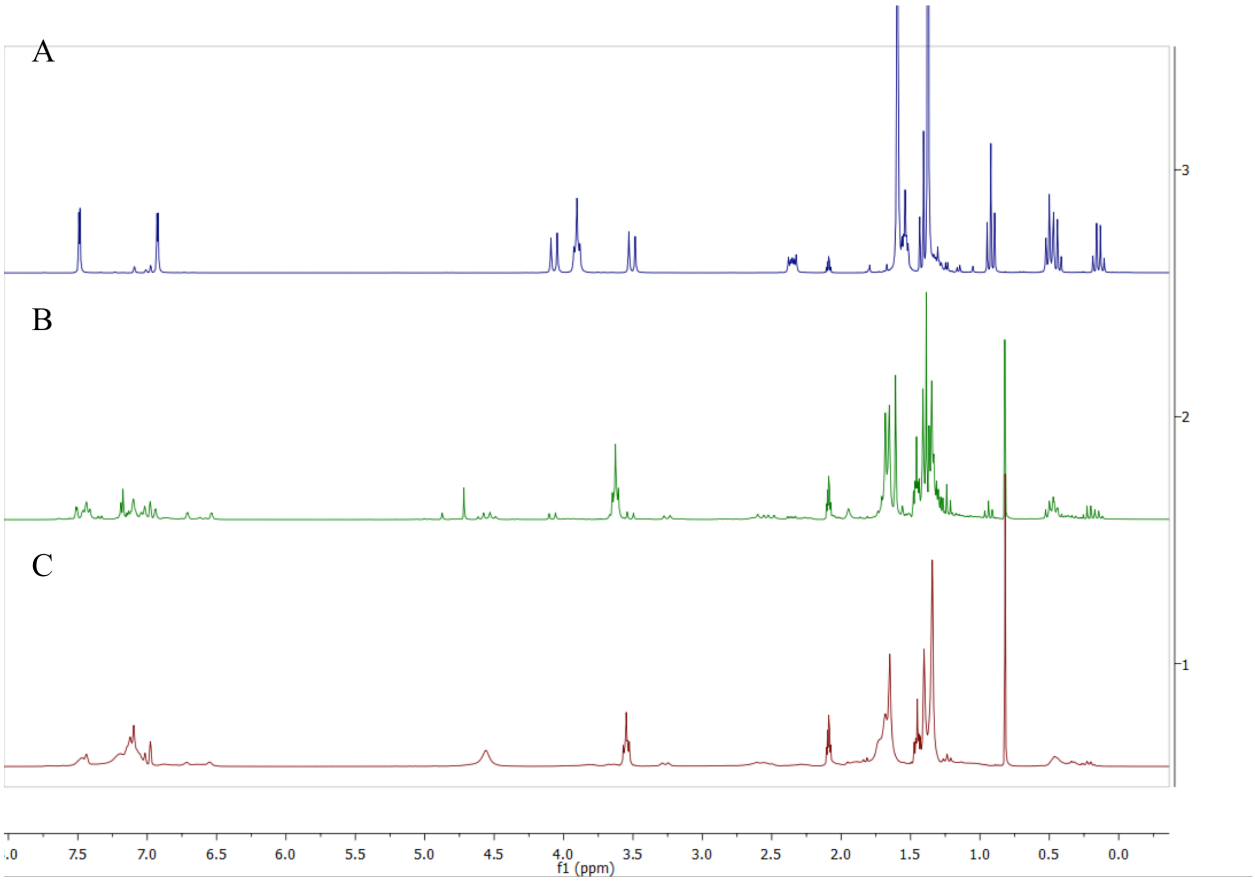

Figure S20. ^{1}H NMR spectra in toluene-d_8 of A: **1a·THF**; B: **1a·THF** with one equivalent BnOH; C: **1a·THF** with two equivalents BnOH.

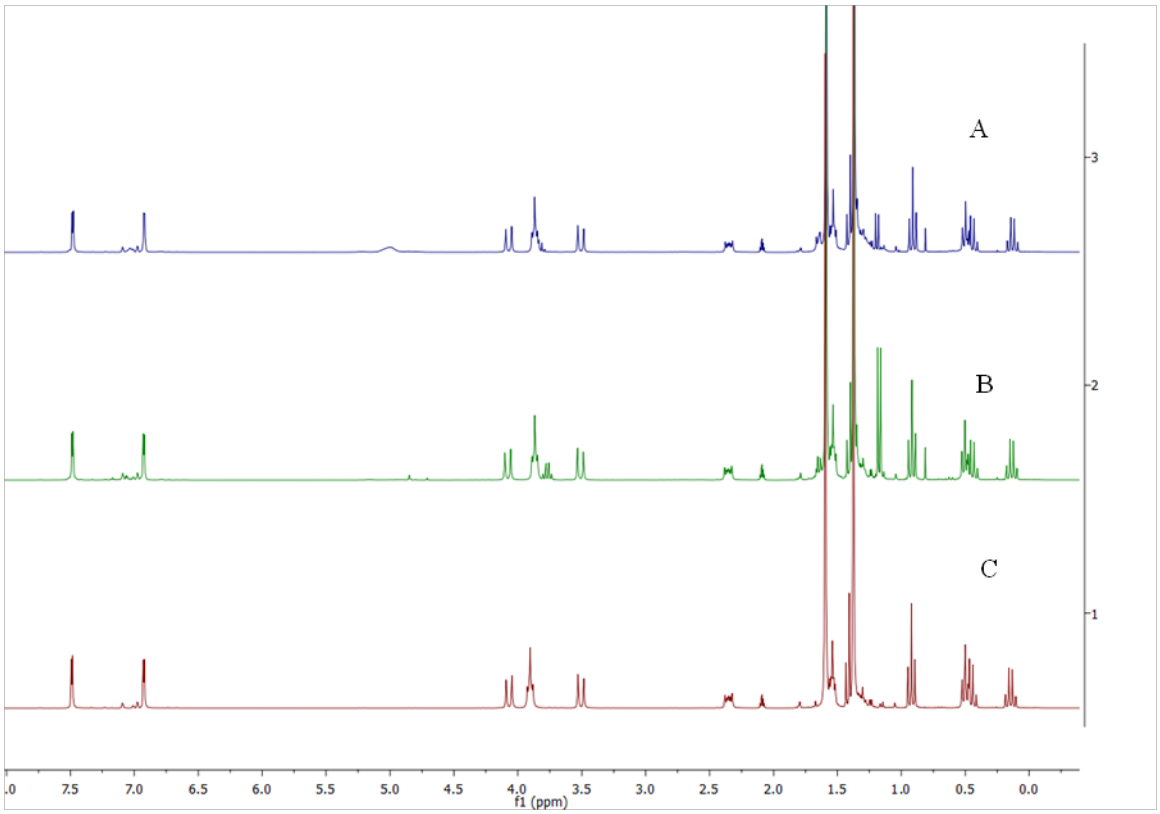

(top)

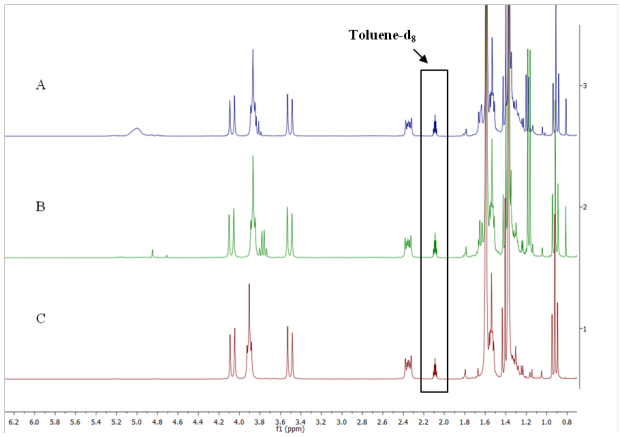

(bottom-left)

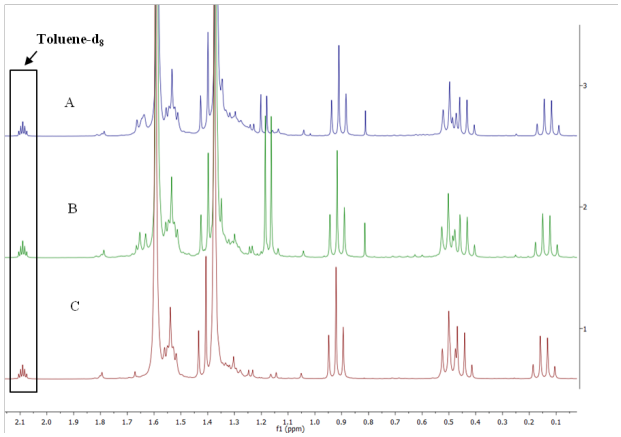

(bottom-right)

Figure S21. Complete ^{1}H NMR spectra (top), expansion of the THF peak region (bottom-left), and expansion of the ethyl group region (bottom-right) in toluene-d_8. A: [LA]:[**1a·THF**]:[BnOH] = 1:1:1 after heating to 353 K for 60 min; B: mixture of [LA]:[**1a·THF**]:[BnOH] = 1:1:1 before heating; C: **1a·THF** alone.

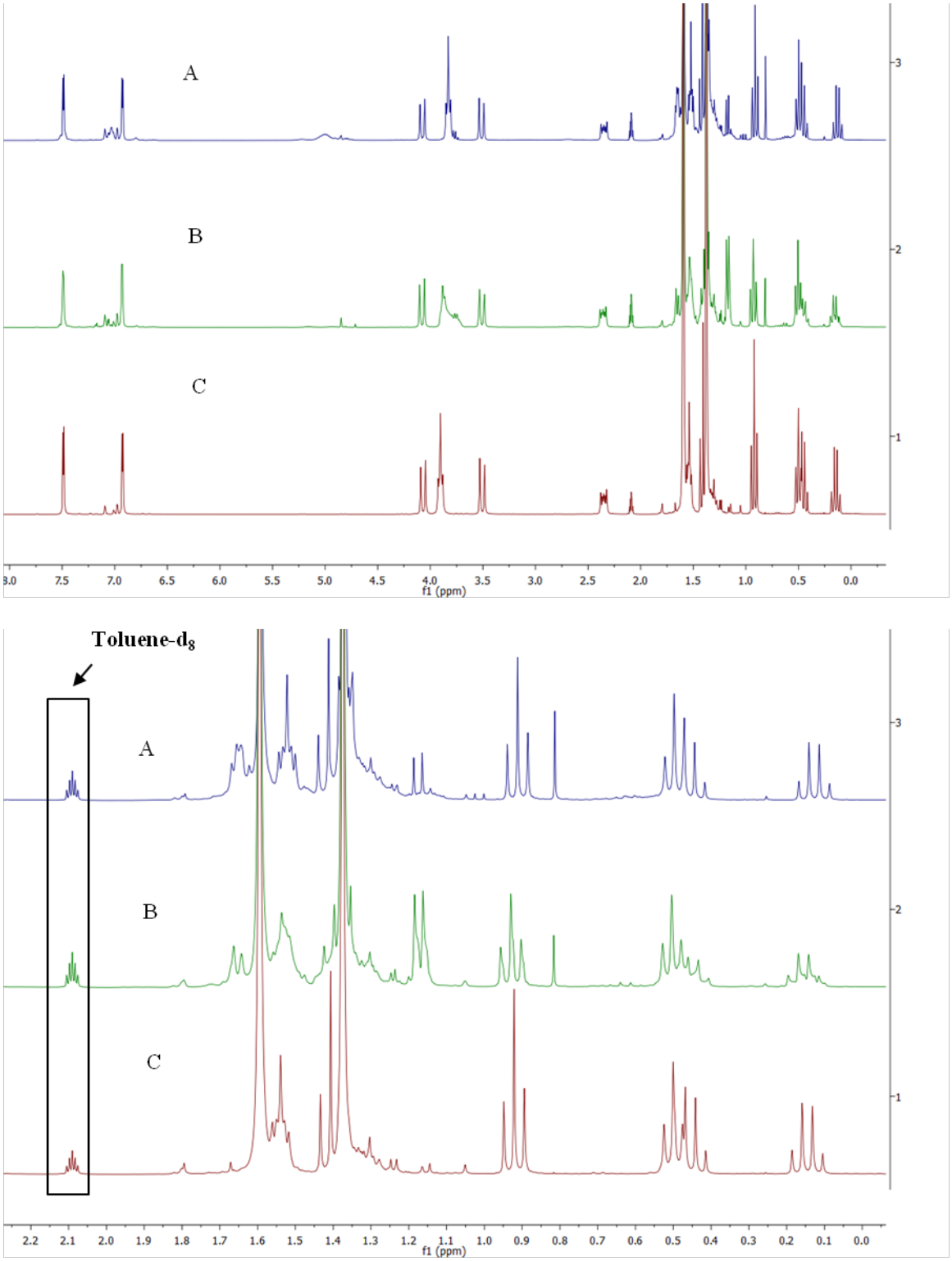

Figure S22. ^{1}H NMR spectra (top) and expanded spectra of ethyl group region (bottom), in toluene-d_8. A: [LA]:[**1a·THF**]:[BnOH] = 1:1:2 after heating for 72 min; B: mixture of [LA]:[**1a·THF**]:[BnOH] = 1:1:2 before heating; C: **1a·THF**.

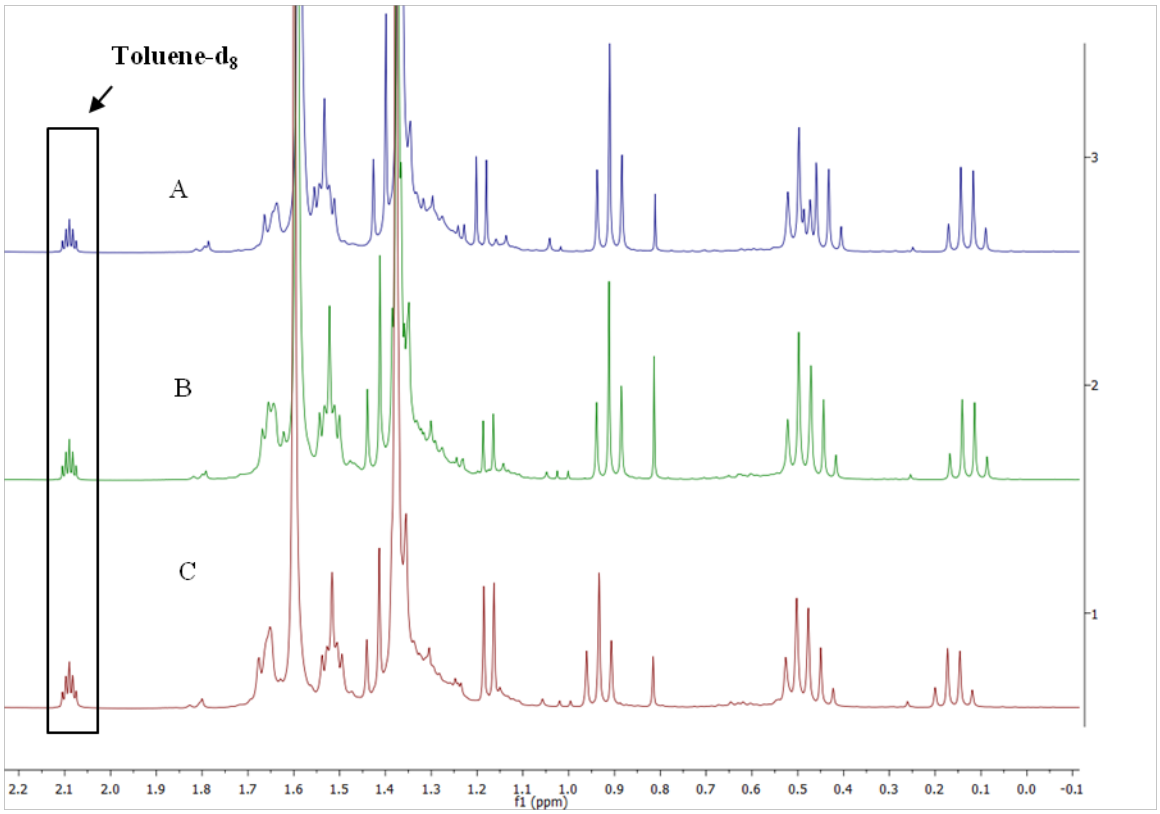

Figure S23. Expanded ^{1}H NMR spectra in toluene-d_8 of A: [LA]:[**1a·THF**]:[BnOH] = 1:1:1 after heating for 72 min; B: mixture of [LA]:[**1a·THF**]:[BnOH] = 1:1:2 after heating for 60 min; C: mixture of [LA]:[**1a·THF**]:[BnOH] = 2:1:1 after heating for 60 min.

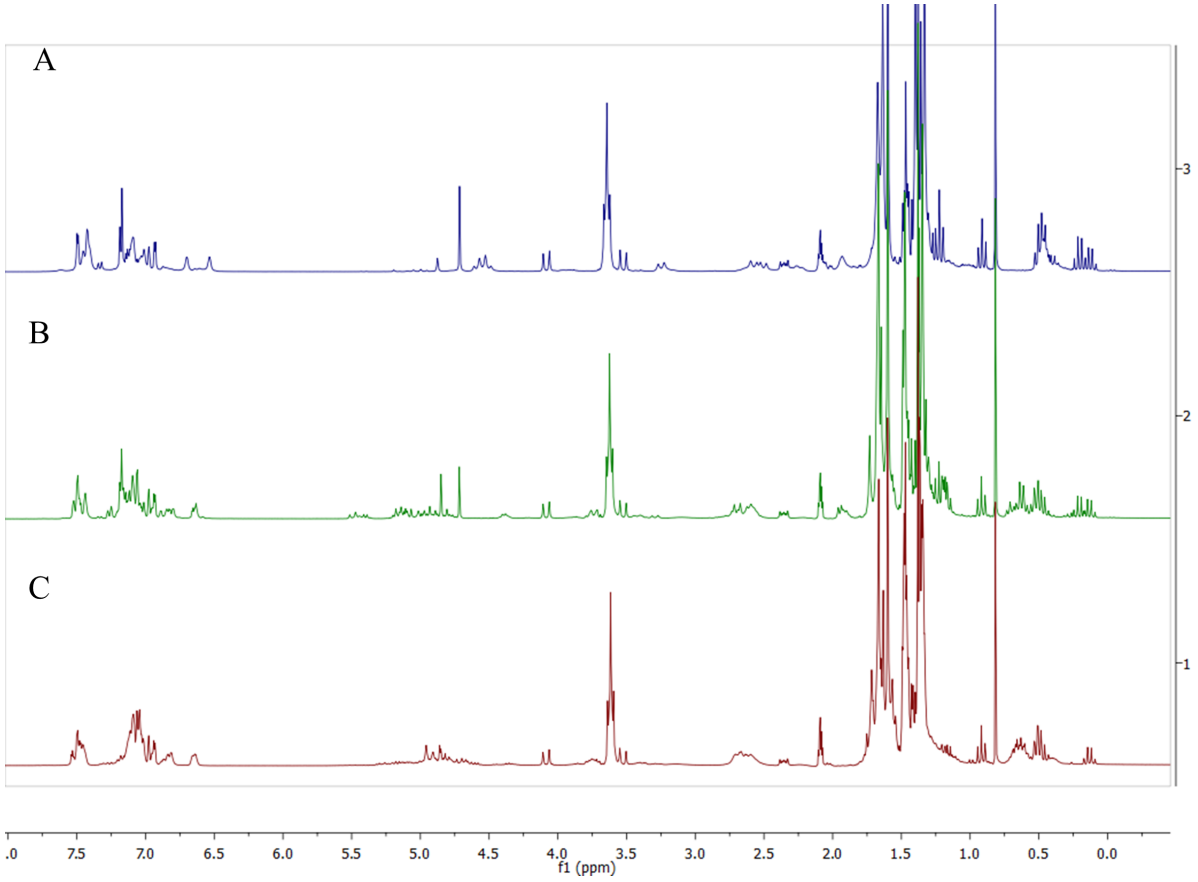

Figure S24. ^{1}H NMR spectra in toluene-d_8, of A: **1a·THF** with one equivalent of BnOH; B: **1a·THF** with one equivalent BnOH then addition of one equivalent of LA; C: the mixture of B after heating for 1h.

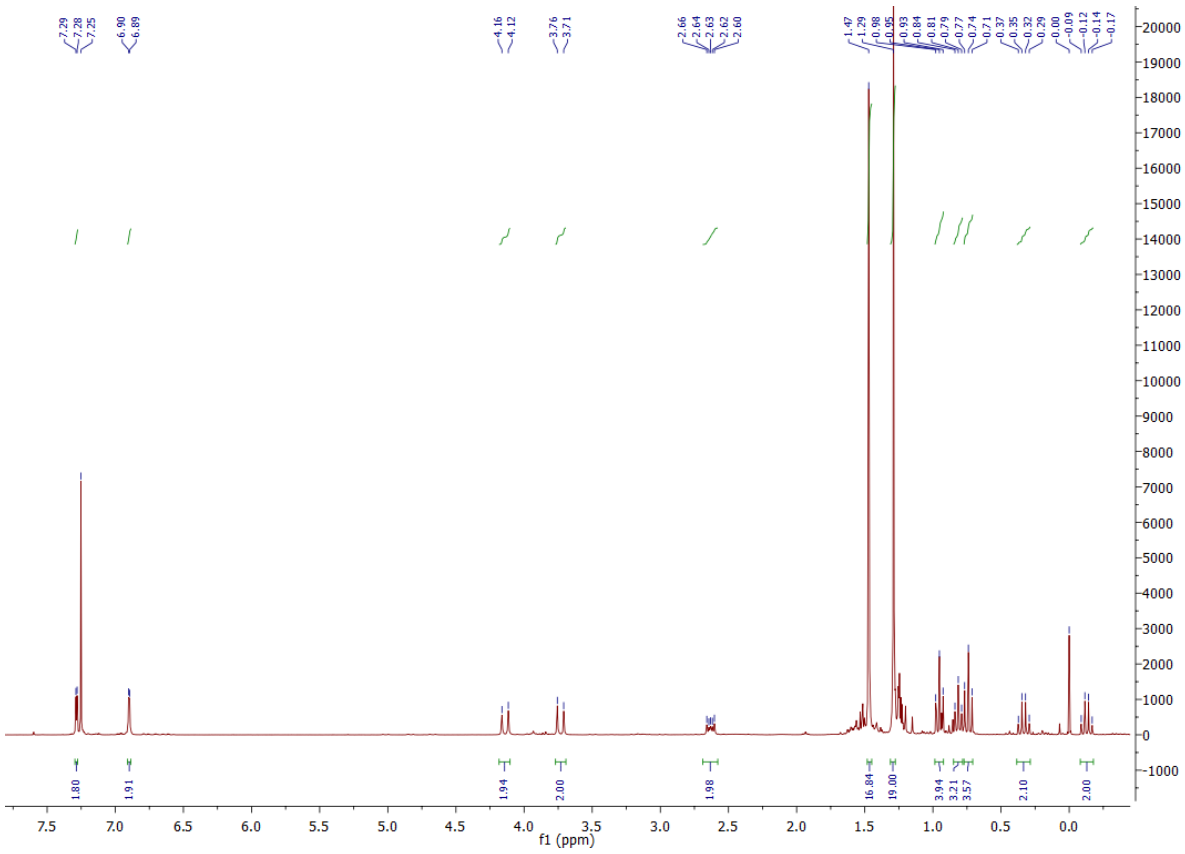

Figure S25. ^{1}H NMR spectrum of **1a** (300 MHz, $CDCl_3$, 298 K).

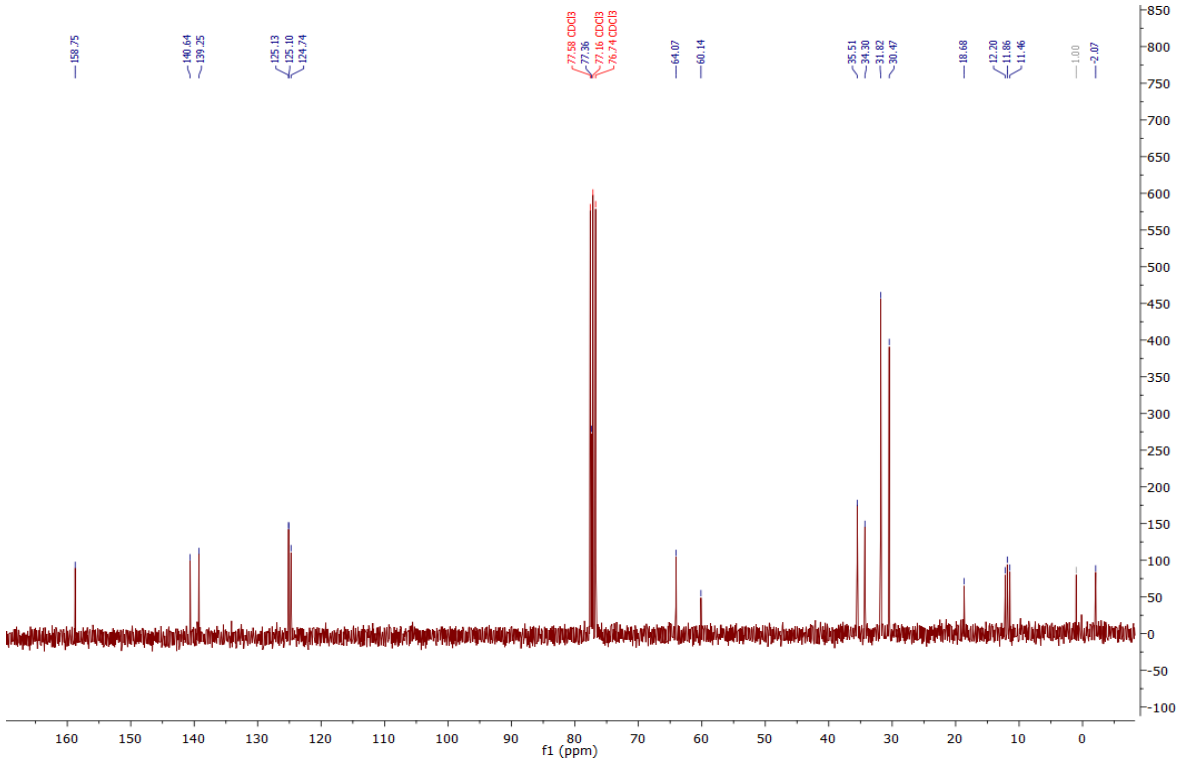

Figure S26. ^{13}C NMR spectum of **1a**, (75.5 MHz, $CDCl_3$, 298 K).

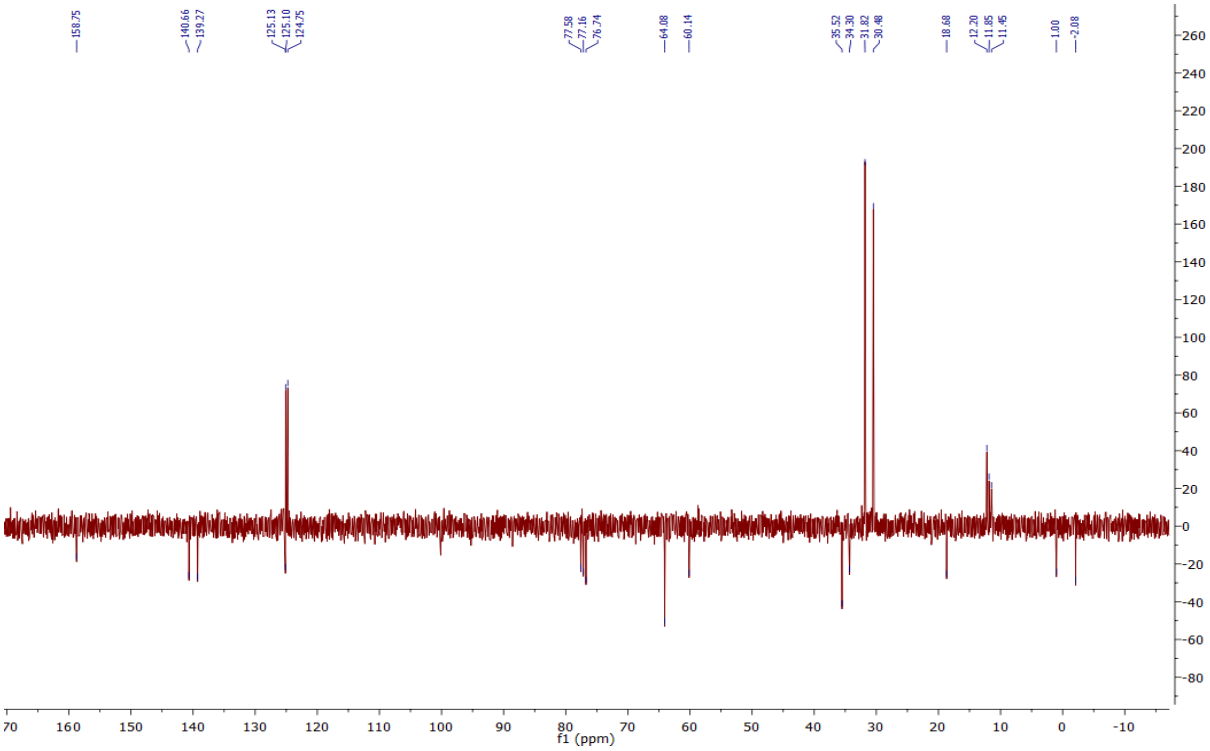

Figure S27. APT (attached proton test) spectrum of **1a** (75.5 MHz, $CDCl_3$, 298 K).

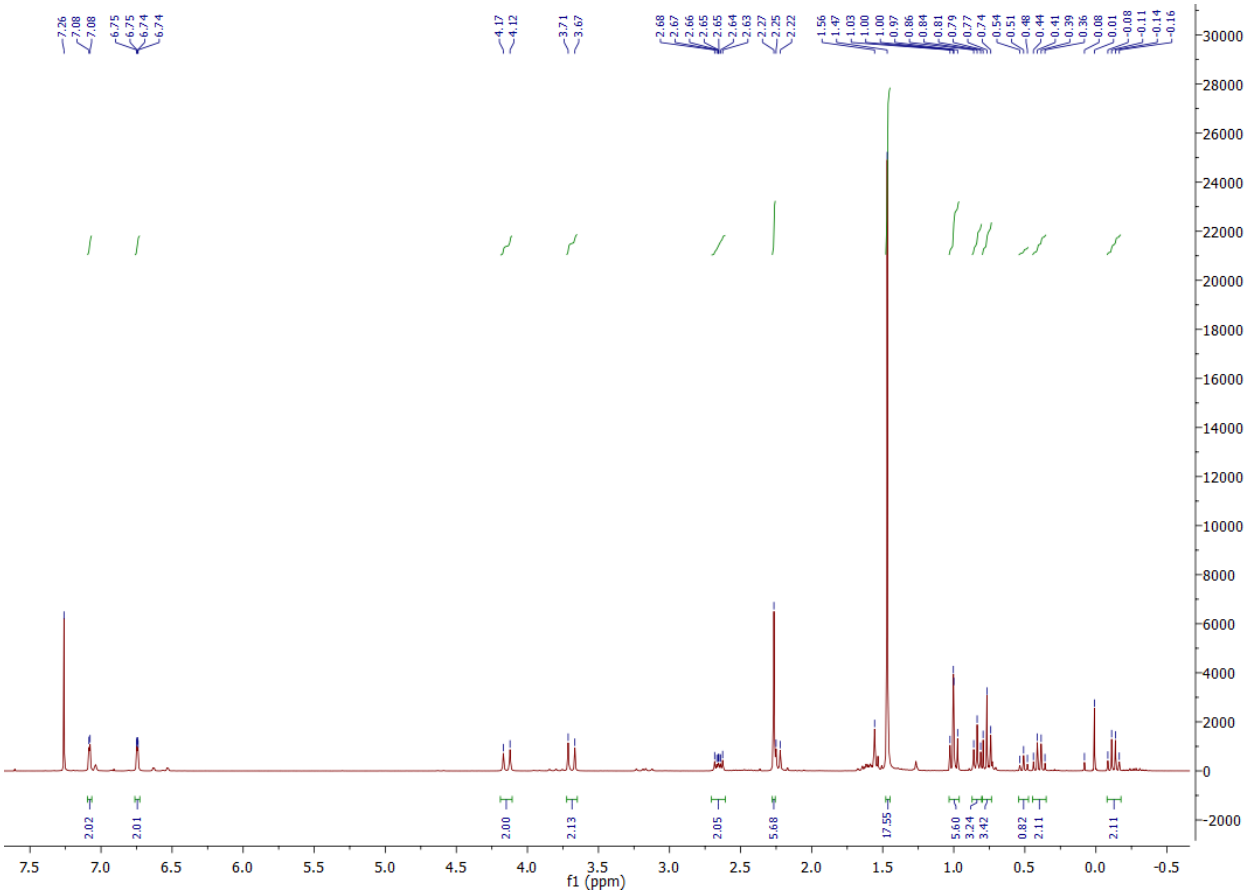

Figure S28. ^1H NMR spectrum of **1b** (300 MHz, $CDCl_3$, 298 K).

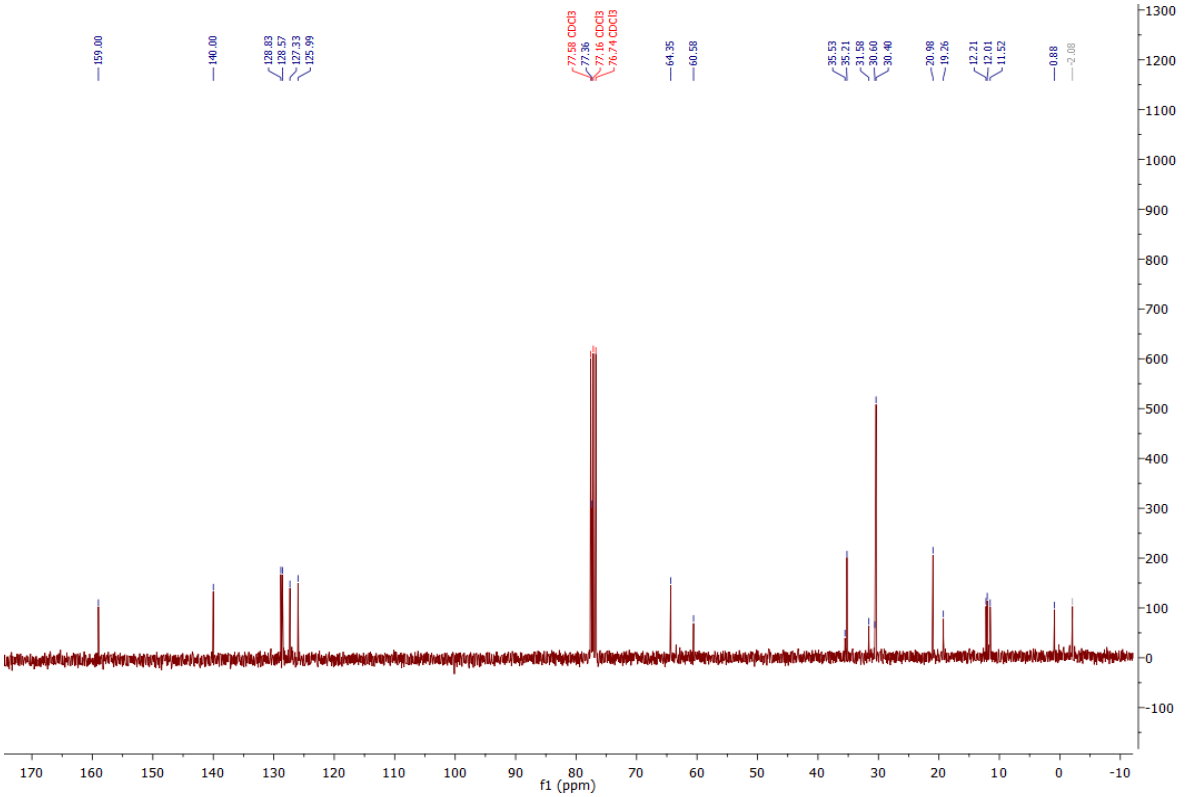

Figure S29. ^{13}C NMR spectrum of **1b** (75.5 MHz, $CDCl_3$, 298 K).

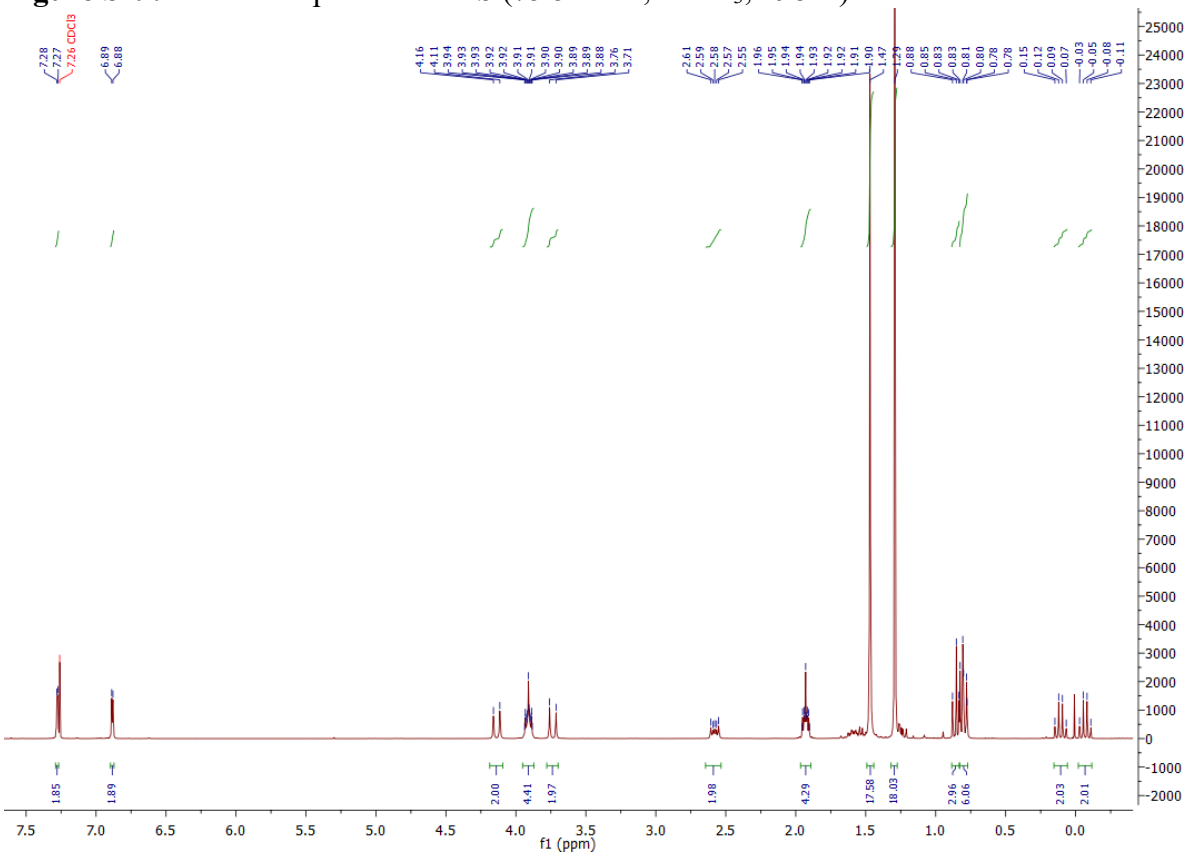

Figure S30. ^{1}H NMR spectrum of **1a·THF** (300 MHz, $CDCl_3$, 298 K).

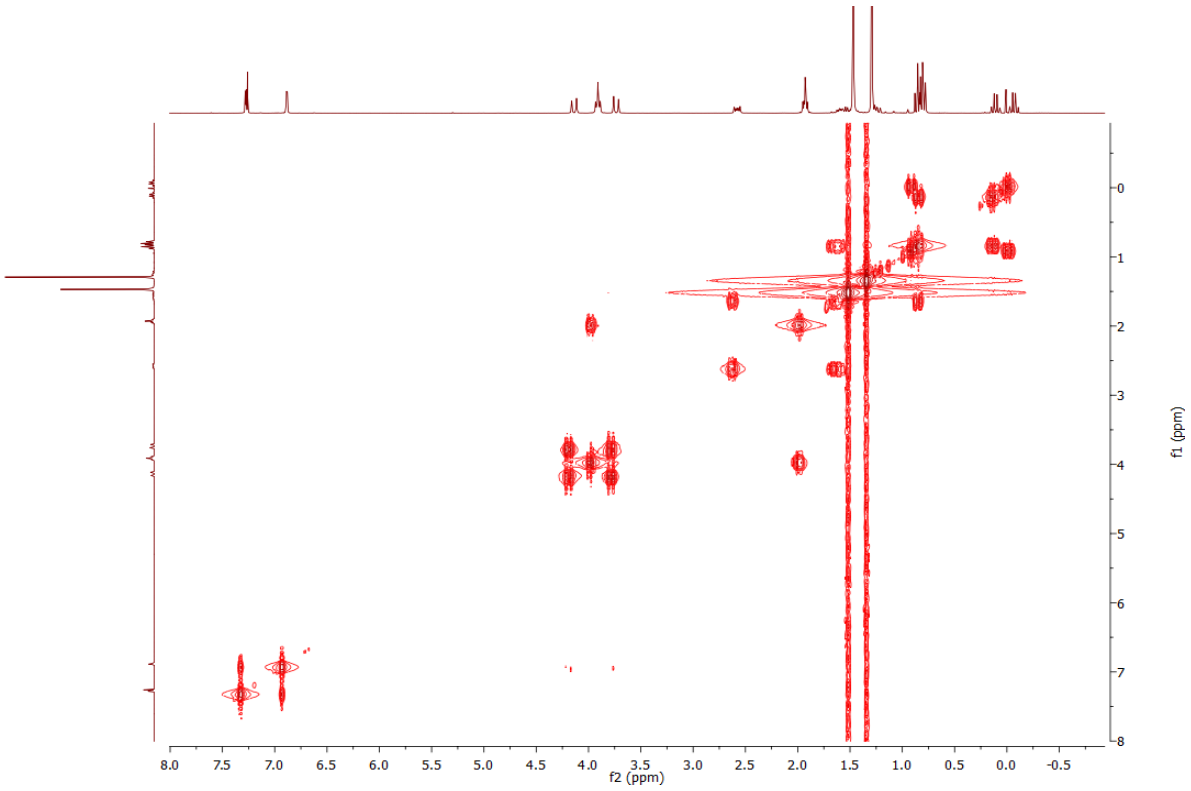

Figure S31. COSY (correlation spectroscopy) spectrum of **1a·THF**, (300 MHz, $CDCl_3$, 298 K).

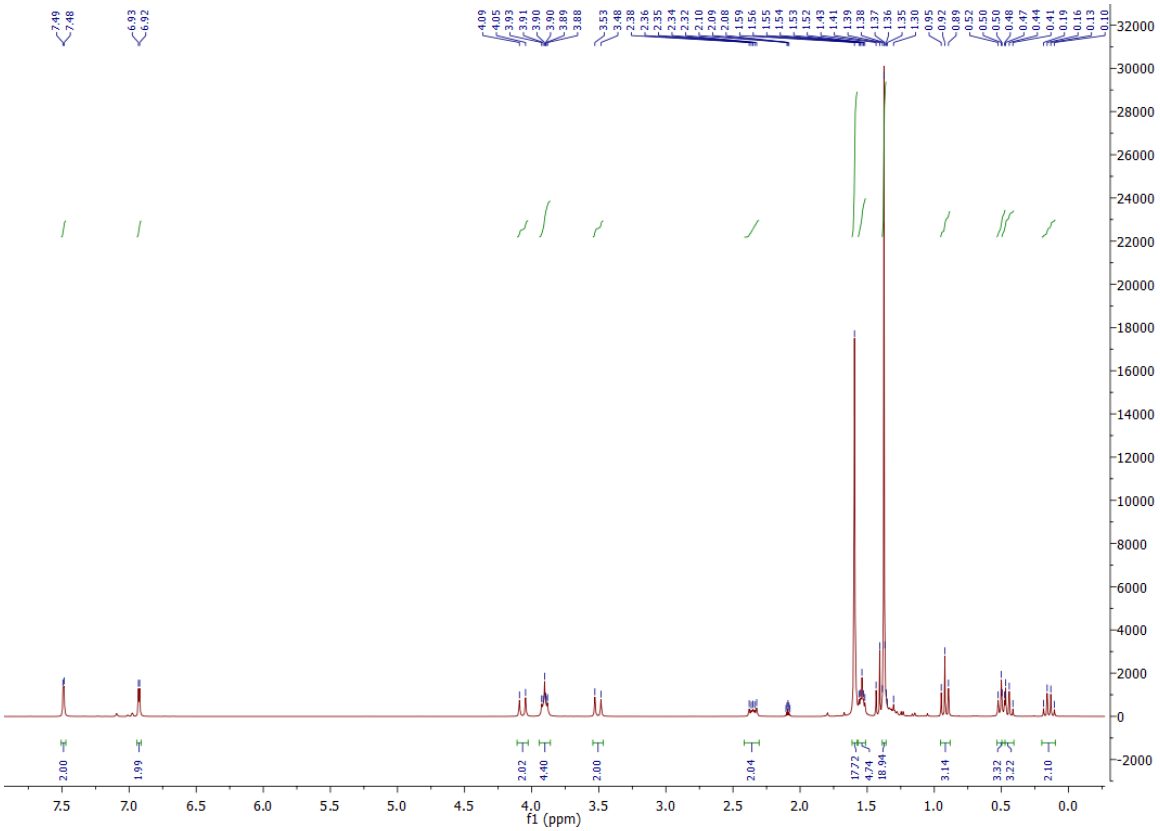

Figure S32. ^{1}H NMR spectrum of **1a·THF** (300 MHz, toluene-d_8, 298 K).

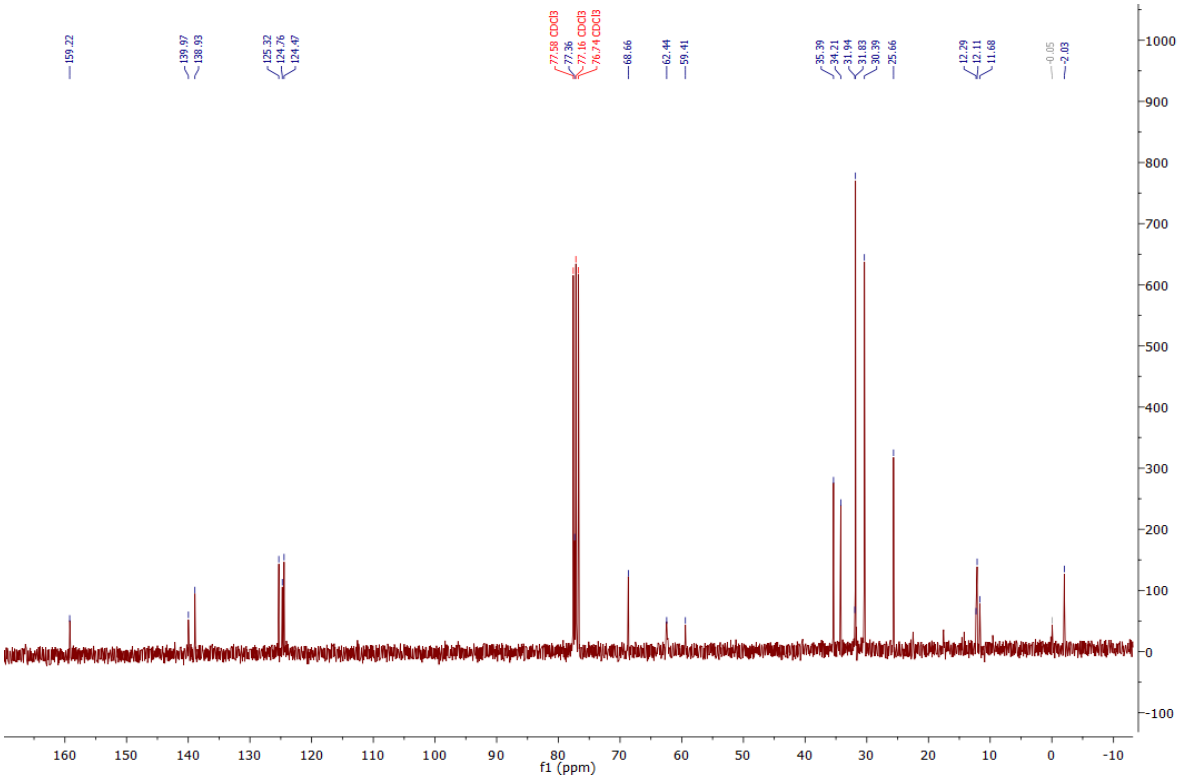

Figure S33. ^{13}C NMR spectrum of **1a·THF** (75.5 MHz, $CDCl_3$, 298 K).

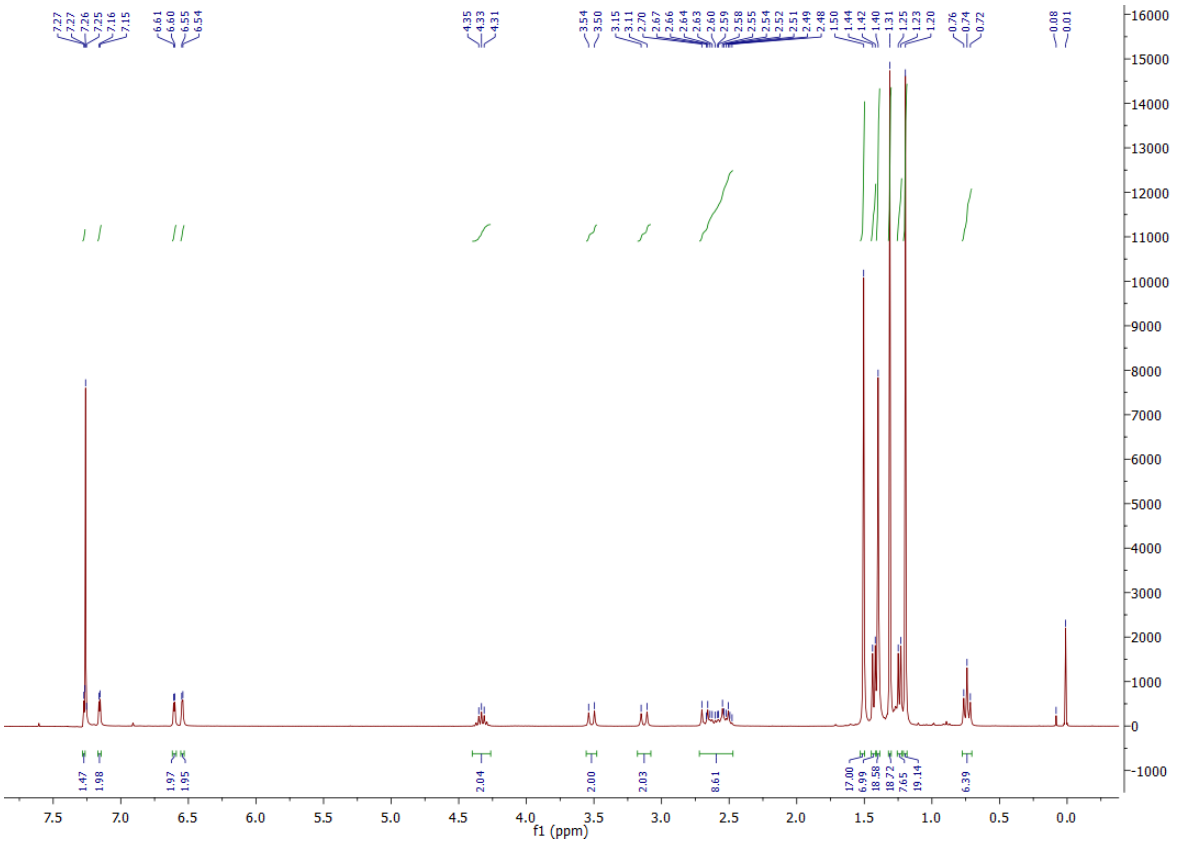

Figure S34. ^{1}H NMR spectrum of **3** (300 MHz, $CDCl_3$, 298 K).

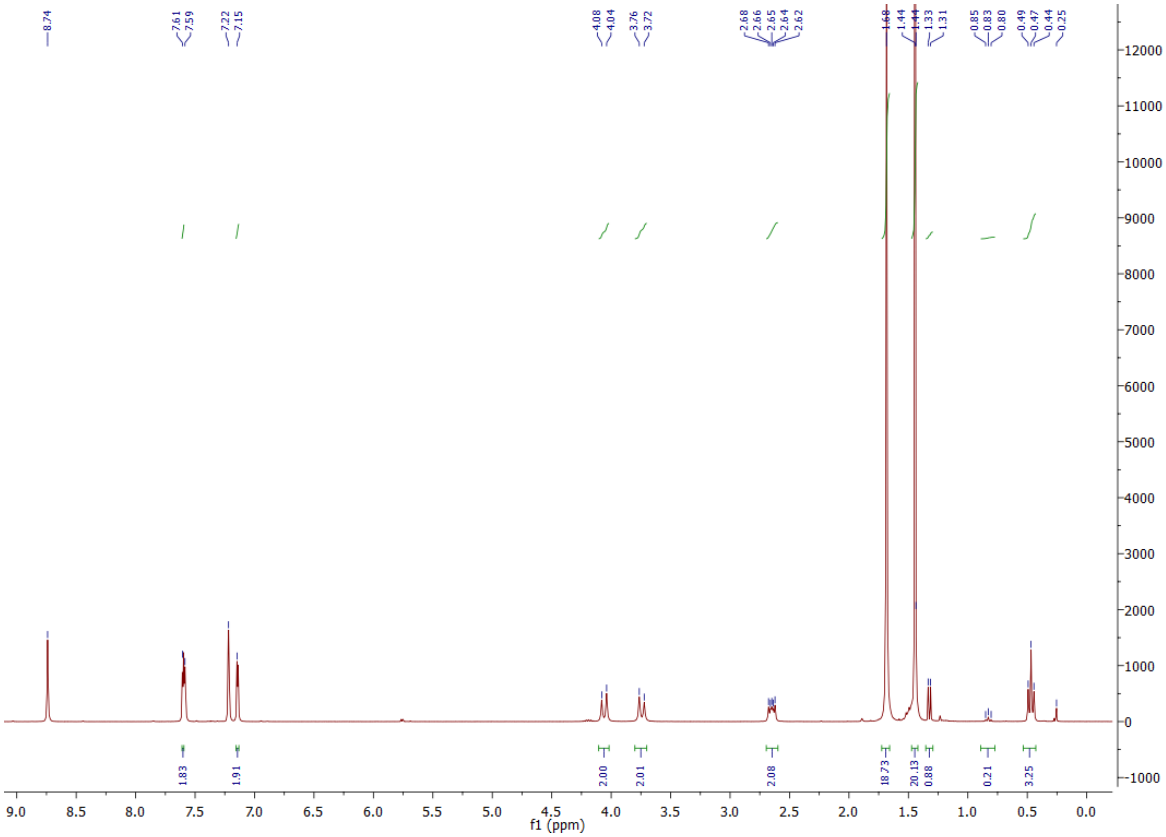

Figure S35. ^{1}H NMR spectrum of **4** (300 MHz, pyridine-d_5, 298 K).

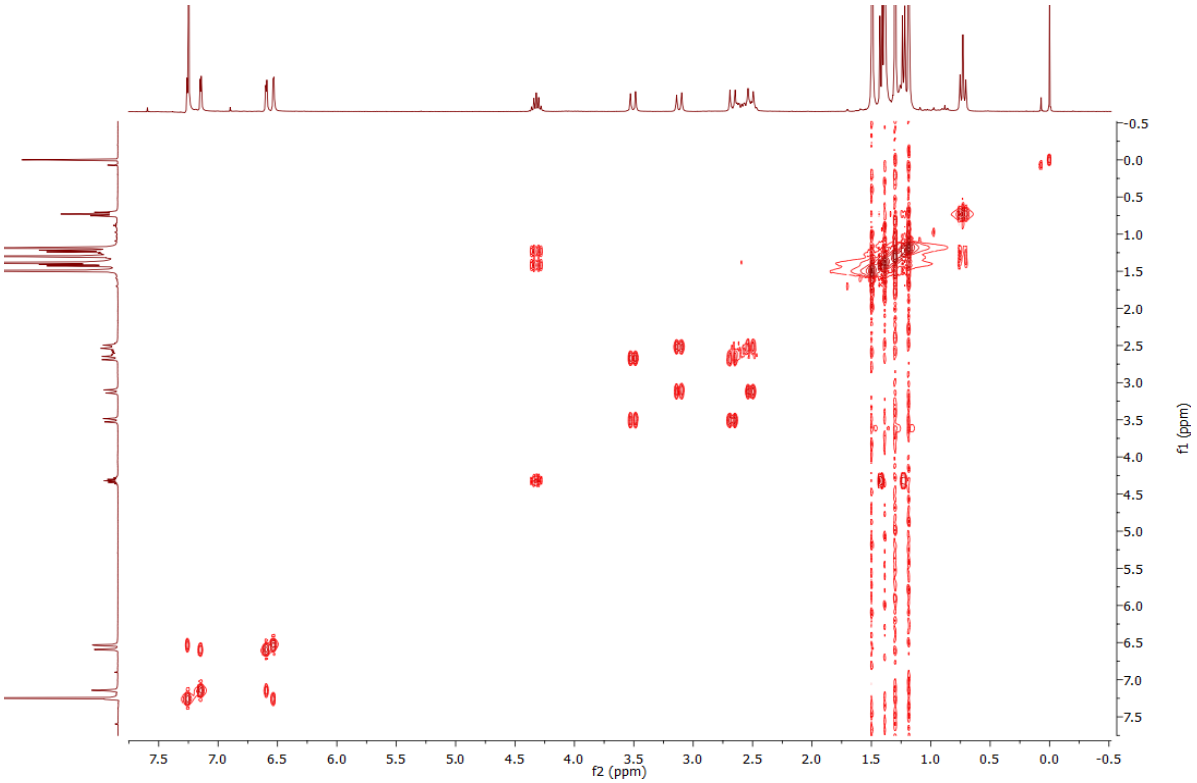

Figure S36. COSY (correlation spectroscopy) spectrum of **3** (300 MHz, $CDCl_3$, 298 K).

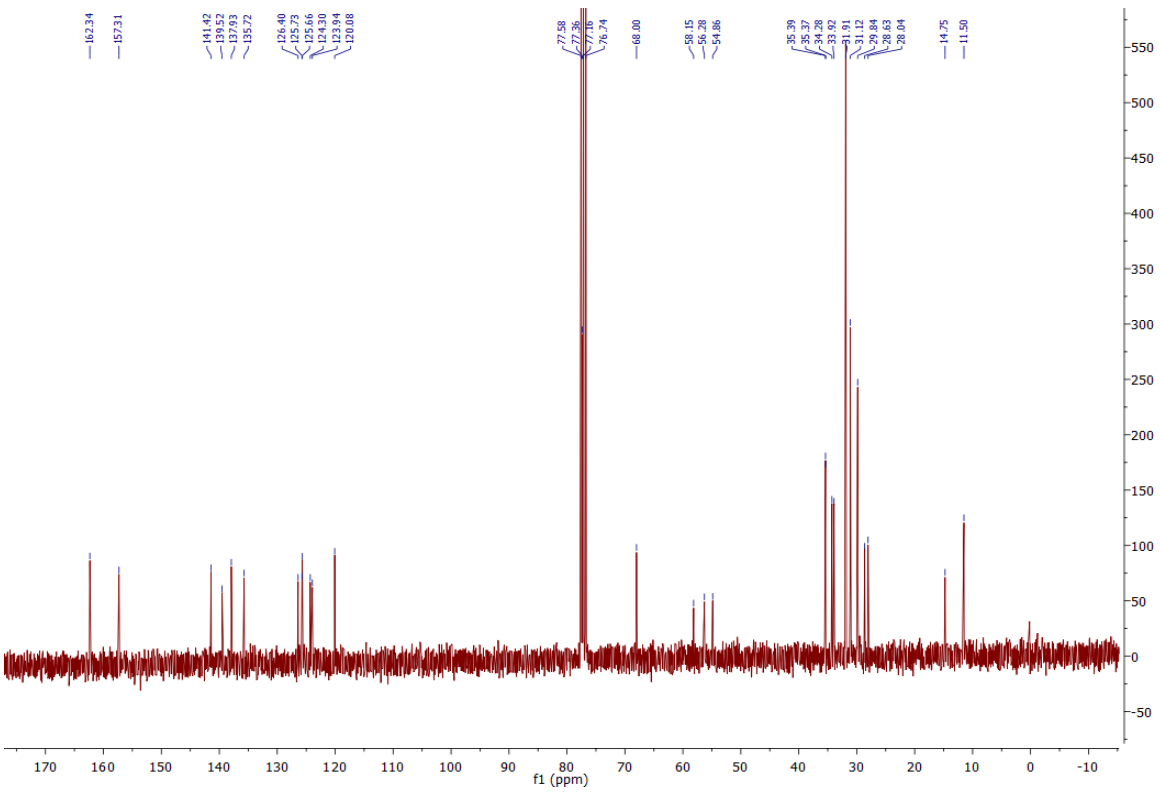

Figure S37. ^{13}C NMR spectrum of **3** (75.5 MHz, $CDCl_3$, 298 K).

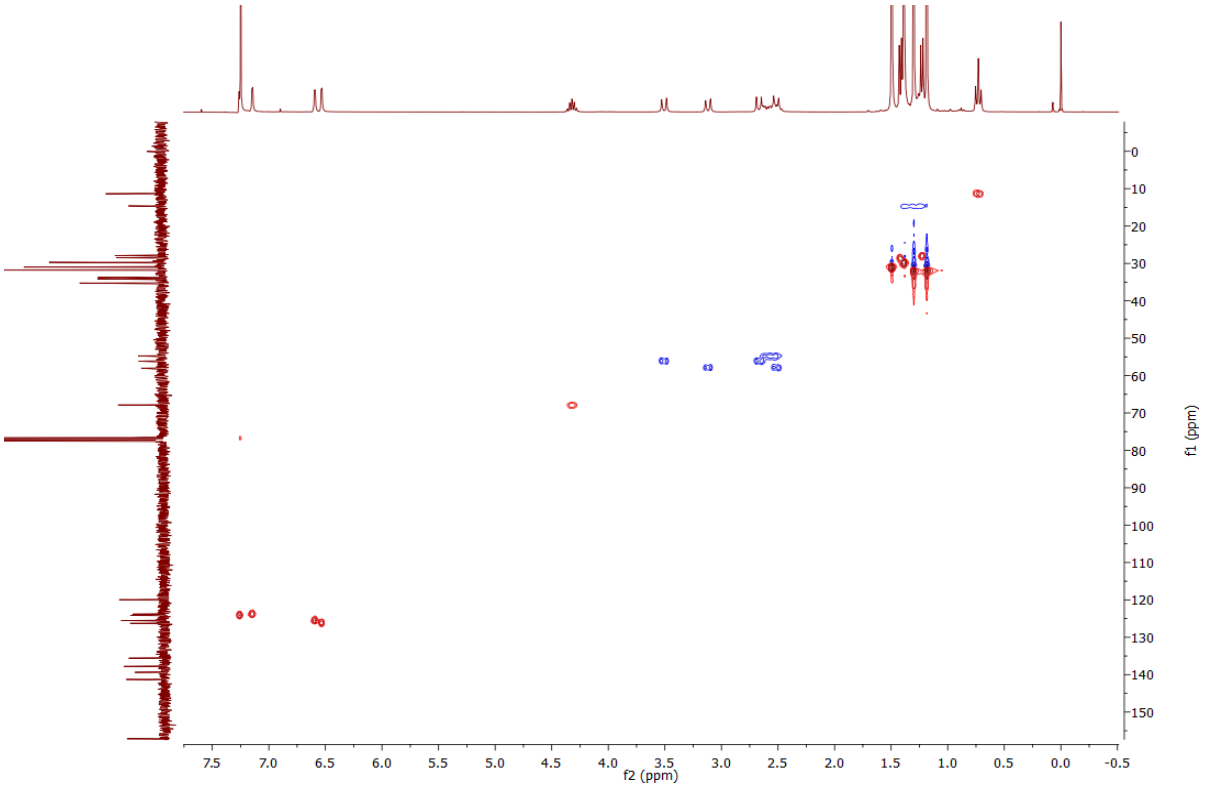

Figure S38. HSQC (heteronuclear single quantum coherence spectroscopy) spectrum of **3** (300 MHz, $CDCl_3$, 298 K).

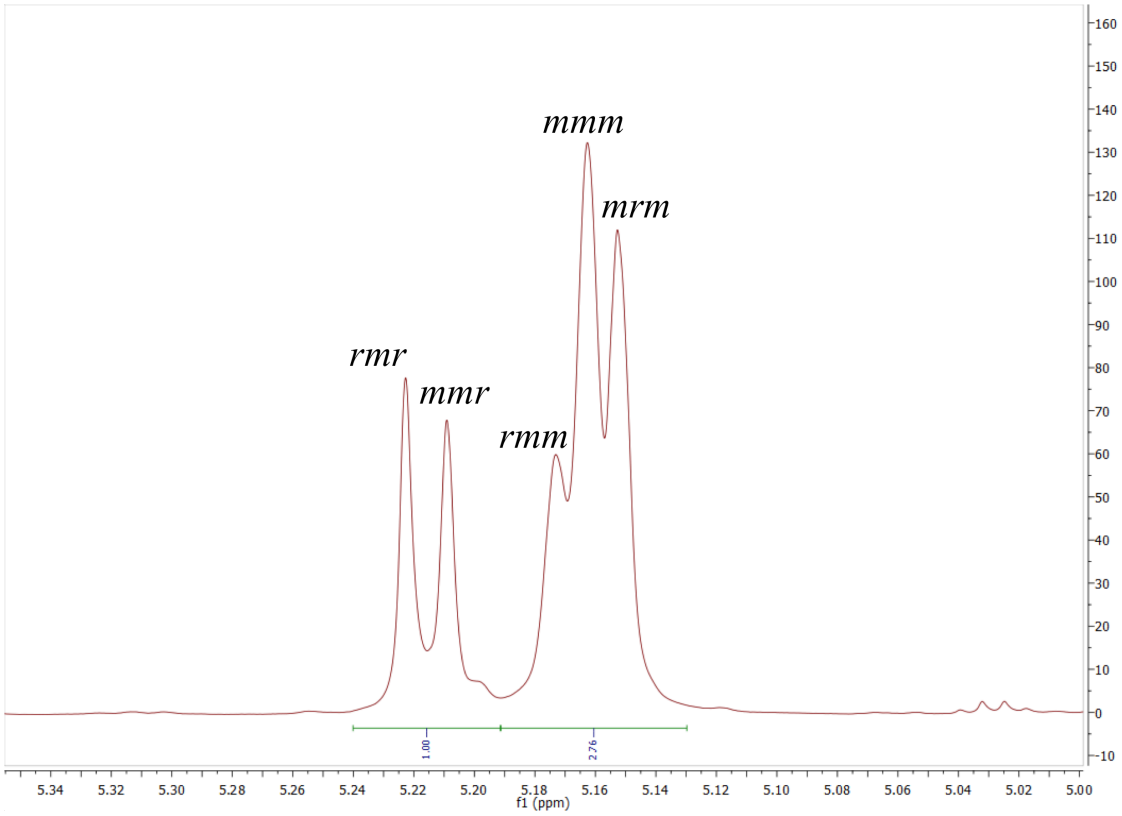

Figure S39. Homonuclear decoupled ^{1}H NMR spectrum of the methine region of PLA prepared from *rac*-LA with **1a·THF**/BnOH ([LA]:[**1a·THF**]:[BnOH]=100:1:1), at 80 °C for 40 min. (500 MHz, $CDCl_3$).